AN EXPERIMENTAL STUDY OF SCOUR AROUND BRIDGE PIERS

by

Tojiro Ishihara

Translated from Journal of the Japan Society of Civil Engineers, Vol. 24, No. 1, 1938, pp. 23-55, Vol. 28, No. 9, 1942, pp. 787-821, and Vol. 28, No. 11, 1942, pp. 974-1005.

Translation by Dr. H. K. Liu, Colorado State University, Fort Collins, Colorado, U. S. A., 1959.

CER47-52TI57

TABLE OF CONTENTS (Part 1)

INTRODUCTION ~~AND ACKNOWLEDGEMENT~~

(1) The Problem of Scour at Bridge Piers

Lately, considerable amount of study, both theoretical and experimental, have been made for formulating a satisfactory basis for designing bridge superstructures. But little work has been reported on the bridge substructure (piers, foundations, etc.) and most designs are based on uncertain design criterions. Hence considerable study can be made on the bridge substructure. This report is a discussion of the bridge substructure design from the hydraulic viewpoint.

Most bridges are closely related to the river. Construction of bridges always changes the characteristics of the stream. It is common knowledge among bridge designers, that serious considerations are necessary in choosing the sites for bridges and piers, and also for selecting arrangement and type of piers. In choosing a bridge site, it is reasonable to select a narrow place in a straight reach of the river channel. The number and arrangement of piers, considering economy, depends on the design of the bridge superstructure. However, design is restrained by hydraulic limitations for flood control and irrigation purposes. Piers should be so arranged that there is enough space between them to drain flood water and pass flowing debris.

Construction of a bridge always causes backwater which is evident from the raising of the water surface upstream of it and the increase in velocity of water through the constriction. These effects disturb the stability of the bed around the piers and hence scour and filling are expected.

Some study on backwater due to piers at flood discharge have been made to compute reasonable values in actual cases. Due to the complication of the phenomena of scour around piers, it is neither easy to solve the scour problem theoretically, nor to observe it in the field. Due to the above reasons, it is regretable that any solution to the scour problem depends only on the experimenter's judgement and not on any theoretical reasoning.

There have been many failures of bridges caused by excessive scour. These failures are due to the errors which the engineers have made in their judgement of scour depth. Scour can be reduced by the following methods:

A. Decrease the number of piers and construct piers such that they are parallel to the centerline of flow, so that disturbance of the flow pattern is cut to a minimum. This not only reduces scour but also decreases the backwater and easily drains flood flows.

B. Form the piers to smooth shapes so that there is a decrease in both resistance to flow and scour.

C. Determine the depth of the foundation by considering the depth of scour and the bearing stress of the bed around the piers.

D. Protect the river bed around the pier, against scour, by a stone apron or piling.

These methods are similar to one another. It is convenient, considering economy, to apply several methods at the same time, thus stabilizing the pier. But all these techniques are based on experience and indistinct judgement. Hence further study is necessary.

(2) The Study of Scour and the Law of Similarity.

Because of the complexity of [illegible] scour [illegible] impossible to solve it with the aid of [illegible] which is mainly based on mathematics. Even [illegible] conclusion is made, they may not be [illegible] cases. By correlating between theory and [illegible] safety factors, conclusions applicable in practice [illegible]

The studies which have been made before are based on the classical hydraulics. Unfortunately, hydraulics had no close relationship with fluid mechanics. So that there was not enough confidence to [illegible] results of

phenomena and systematic studies on the structures and models also lead to valuable conclusions which may fit both actual cases and theoretical solutions. This will increase the rate of progress in modern hydraulics. It is necessary for any experimental study on the scour problem to be based on modern hydraulics so that we can get suitable data which can be applied in the field.

The laws of similarity are most important in modern hydraulics. In our case, three of the laws of similarity are applicable;

A. Froude law of similarity - assuming water is incompressible, water particles have an inertia and a gravitational force.

B. Reynolds law of similarity - considering the inertia force and capillary attraction.

C. Weber law of similarity - considering the inertia force and capillary attraction only.

Applying these laws, the close relationship between theory and an actual case in the field and the importance of model tests are recognized.

Table 1. The Model Ratio by Using the Laws of Similarity.

If the ratio of length of ~~structure~~ prototype to length of model be 1:λ and assuming the same fluid having the same temperature, the model ratio for each physical characteristic is as shown in Table 1. But in an actual case, many forces are acting on a fluid particle. It is impossible (observing from Table 1) to find the law of similarity considering these factors at the same time. For this reason, in general, one important force was considered (except inertia force) and the law of similarity which fits this force was applied. e.g. For hydraulic phenomena in open channels the Froude law of similarity was applied. This is because a gravitational force is important besides an inertia force. But, in experiments, it is difficult to use models which have large values of mean hydraulic radius. On the other hand the effect of frictional force overshadows the hydraulic phenomenon in models having small values of the mean hydraulic radius. In this case, it is not sufficient to use only the Froude law of similarity. Mr. Otsubo tried to equalize the coefficient of frictional resistance at similar points in two channels which were geometrically symmetrical. But the coefficient of frictional resistance is affected by the roughness of the channel, mean hydraulic radius and Reynold's number, etc., so that it is impossible to equalize these coefficients. For compensating for this fact, he proposed multiplying the ratio of these two coefficients to the Froude law of similarity. The above statement is applicable only to the case of a fixed river bed. For experiments on scour, it is related to velocity, discharge,

and the size and type of bed material. Accordingly, it is difficult to establish a complete law of similarity and also difficult to predict accurate scour in the field ~~from the field~~ from the results of experiments. For the above reasons, Winkel, Krey, Eisner and Vogel proposed to establish an approximate law of similarity for practice instead of using the theoretical law of similarity.

(3) The Purpose and Content of this Report.

Lately considerable progress on the study of the scour problem has been made by applying the law of similarity, yet it is far from completion. In this paper, the results of experiments which were made at The Central Experiment Station at Kyoto University have been reported. Conclusions derived from the study have also been stated.

Chapter 2 is a discussion on the stability of a river bed with basic ideas for model tests on the scour problem. In Chapter 3 the effect of pier ~~type~~ shape on scour has been discussed. This is the main subject of this report. ~~The last part of this report is a description of the effect of pier arrangement on scour.~~

~~Concerning the mechanics of scour and its protection,~~ the results of experiments performed by authorities in the subject and some of the author's opinions regarding them have already been stated in this report.

Because of the lack of coincidence between the model and prototype data, resulting from imperfections in the law of

for the prototype
similarity, no accurate conclusions can be obtained from the experimental data, but further study for correlating experimental work with actual field conditions is expected.

II. THE STABILITY OF A RIVER BED AND THE RELATIONSHIP BETWEEN TRACTIVE FORCE AND BED MATERIAL

(4) General

It is impossible to solve the problems on the movement of bed material from the theoretical view points of fluid mechanics, especially, ~~if~~ at the same time the stability of a river bed is discussed. Based on a hydraulic study, At the present day, therefore, it is based mainly through experiments, there are two methods to solve the problems of sediment movement.

A. The method based on the impulse force caused by velocity near the bed.

B. The method based on the theory of tractive force.

In general, if there is relative velocity between a fluid and solid, dynamic pressure acts on the solid in the direction of the relative velocity. This is mainly due to frictional resistance and form resistance. The former is due to fluid friction and is related to the surface area of contact between the solid and water, roughness of solid surface, relative velocity, and the viscosity of water. The latter is due to the pressure difference between the front face and the rear face of the solid, and is related to the shape of the solid and the relative velocity of the fluid. If the density of fluid is $\frac{\omega}{w_0}$, the relative velocity is V and the projected area of the solid on the normal plane to the direction of flow A,

dynamic pressure P is

$$P = \beta \gamma_0 A \frac{V^2}{2g} \text{ - - - - - (1)}$$

in which where β is an experimental coefficient. This coefficient is a function of Reynold's number, $R = \frac{V\ell}{\nu}$, especially, when the dynamic pressure is mainly due to frictional resistance; if the dynamic pressure is maily due to form resistance and the solids are similar, β has an approximately constant value for any kind of any similar solid and fluid.

For a sand particle at a state of rest on a bed, the relative velocity is equal to the velocity of flow. If the dynamic pressure exceeds the resistant force, the particles start moving and scour occurs.

The resistant forces of the particles are different for sliding and rolling. Most particles move in the path of least resistance. The particles having a flat or a square shape will slide and the particles having a spherical or cylindrical shape will roll. This is a study (general idea) of the (method based on the) impulse force of velocity. At limitations of a stable bed, the diameter of the sand particles is expressed as $d = f_1(V)$, in which V is the velocity of flow acting on the particle. This theory originated from Newton's dynamic pressure theory and was studied by Brahms, Airy and Law.

The theory of tractive force was proposed by Du Buat and expanded by DuBoys through observations on the River Rhome. Kreuter and de Thierry published the theoretical explanation but it still seems incomplete. The main assumption is that, in uniform steady flow, the gravity component of the weight of water parallel to flow is balanced by frictional resistance

on the bed, and this resistance force is equal to the tractive force on the bed surface.

The tractive force F, in kg/m^2, can be written as:

$$F = W_o H I \text{ - - - - - (2)}$$

where: H = depth of flow,

I = slope of the water surface = slope of the bed surface

W_o = weight of a unit volume of water, kg/m^3

The stability of a river bed will decrease with increasing tractive force. According to the theory of tractive force, critical tractive force F_o is constant for each different size of bed material. Within the limitation of bed stability, the diameter of a sand particle can be expressed as:

$$d = f_2 (F_o) = f_2 (H.I).$$

In these two methods, the former uses velocity V as the basic characteristic of flow and the later takes slope, I, and depth, H, as basic characteristics of flow. Comparison between the two theories have been made by many authors. H and I are easy terms to measure in the field, also it is convenient to apply the theory of tractive force for engineering purposes since H and I can be measured more accurately than velocity near the bed or the mean velocity. These two methods were established only for solving problems and there is no essential difference between them, moreover, they are closely related. Theoretically speaking, tractive force is considered as shear stress, $\tau_w = \rho \left|\frac{dv}{dy}\right|_{y=o}$, on the bed and is determined by the velocity distribution in the boundary layer. Accordingly, tractive force

is affected by Reynold's number and the roughness of the river bed. On the other hand, the dynamic pressure of the sand particle is mainly controlled by velocity and its distribution near the bed in the boundary layer. Hence we can observe the close relationship between the two theories. Although a precise correlation between the two theories is essential in studying the mechanics of particle motion, no complete correlation has been reached. Hence it is difficult to apply, in the field, the experimental results on the study of particle movement.

(5) The Stability of a River Bed Based on the Impulse Theory of Velocity near the Bed Surface

A. General

Dynamic pressure on a sand particle by velocity V_b is as in equation (1). When the resistance of a particle is less than the dynamic pressure, the particles begin to move and scour occurs.

At the limit of stability of a river bed, assuming a particle resting on a rigid surface, the relation between mean diameter of sand particle d and velocity near the bed V_b is mathematically expressed by the following equation:

$$d = KV_b^2 \quad ; \quad K \approx \frac{1}{10} - \frac{1}{15} \text{ - - - - - -(3)}$$

The coefficient K is related to the shape of the particle, its position, the velocity distribution near the bed, the Reynold's number and the roughness of the bed.

Brahms (1753) used the weight of a particle in water W_1 instead of the mean diameter of particle d and stated the condition of sliding as $V_b = f, W_1,^{1/6}$. This equation was veri-

by Airy (1834) and Law (1885). Law also stated that this equation could be applied for rolling particles. Steinberg (1875) assumed sand particles as rolling particles having similar shape and mean diameter, 2a, and noted $V_b = \sqrt{2a}$.

In actual river beds, the sand particle is surrounded by other particles having approximately the same size. The part in contact with the fluid is only the upper half of the particle. Therefore, the coefficient in Eq (3) should decrease. Since the velocity near the bed is extremely low, the determination of V_b becomes a difficult problem, moreover, consideration of the size of particle and other factors is required. There were many experiments made by du Buat (1816), Suchier (1883), Franzius (1890), Schaffernak (1922) etc. Herein is a discussion of Schaffernak's work. By obtaining a relationship between velocity near the bed and the mean velocity of flow and also expressing the mean velocity by the Chezy formula, the relationship between the Impulse Theory and the Tractive Force Theory can be examined by hydraulic methods.

B. Schaffernak's experiment.

By using a small experimental flume with sand of uniform size, he found the relationship between velocity V_b and mean diameter d as listed in Table 2.

TABLE 2

Diameter of particle, d cm.		
Particle starts moving V_b m/sec.	(V_o)	
Particle continues moving "	(V_1)	
Particle Stops moving "	(V_2)	

Approximately $V_o \doteqdot 2V_2$, $V_o \doteqdot 1.5V_1$, $V_2 \doteqdot \frac{3}{4} V_1$

C. Welikanoff's experimental formula

The dynamic pressure on a sand particle is proportional to the second power of velocity. But it is still doubtful whether this proportionality can be applied to fine sand particles. The velocity in the boundary layer decreases rapidly near the bed and in case the velocity is large enough, in magnitude, to move large particles, the boundary layer becomes thin and ~~particles are controlled~~ the dynamic pressure on a sand particle is governed by the velocity outside the boundary layer. But in the case of fine particles, this phenomenon is contrary to observations. ~~Hence~~ that for the case of large particles the determination of velocity near a bed must change with the size of particles. If a theoretical determination of the velocity distribution near a bed, ~~according to the size of particles,~~ is possible, a theoretical solution of V_b can be expected. At present, we still rely on experimental results. Welikanoff used a $50^{cm} \times 25^{cm} \times 900^{cm}$ flume with sand size, $d\phi$= 0.01 - 5.0 mm, and established an experimental formula relating the diameter of sand particles and the mean velocity of flow.

$$\frac{V^2}{g} = \alpha d + \beta \qquad \text{------ (4)}$$

where: g = gravitational acceleration (mm/sec^2)

V = velocity of flow (mean), (mm/sec)

d = mean sand size (mm)

α, β = experimental coefficients

When the whole sand layer starts moving,	$d \leq 0.5$ mm	$\alpha = 0.65$,	$\beta = 11.0$
	$0.5 < d < 5.0$ mm	14.0	5.8
when each particle starts moving	$0.01 < d < 5.0$ mm	7.3	3.0

when the sand particle is larger than 2 - 3 mm, β is neglected and the formula becomes

$$\frac{V^2}{g} = 14\, d$$

By using sand with diameter d = 0.01 ~ 1.00 mm, Welikanoff made experiments relating depth of water H and β found that β increases with increasing H

$$\beta = 0.051\, H + 5.7 \text{ for } H = 25 \sim 150 \text{ mm} \qquad (41)$$

His experiments proved that the thickness of the boundary layer changes with depth of flow and the movement of fine sand particles is evidently controlled by the velocity in the boundary layer.

(6) The Stability of a River Bed Based on the Tractive Force Theory

A. General Study:

The following conclusions can be made from the study of the critical tractive force, F_o: In open channels having common slope $(\frac{1}{400} - \frac{1}{800})$ with certain size material, the stability of the bed surface is determined by the critical tractive

force for that size of material, and cannot be determined by the depth of flow or slope alone. Kreuter (1898) reached this conclusion through investigations in natural rivers and Schaffernak (1916), Gilbert (1914), Schoklitsch (1914) and Kramer (1934) verified his findings through flume experiments.

The critical tractive force can be determined by the characteristics of the bed material but it is impossible to compute it by using only the diameter of the sand particle or any other numerical value which represents the particle size. From Gilbert and Kramer's experiments, it is seen that critical tractive force is a function of the size of particle and its distribution, the shape of particle, the consistency of the sand layer and the specific gravity of the sand particle.

The size of a particle and its distribution can be obtained by sieve analysis. The shape of particles can be obtained by precise measurements but the shape of common river sand composed of quartz can be considered as approximately constant spherical. The consistency of the sand layer can be obtained by measuring the void ratio. Therefore, critical tractive force can theoretically be expressed by the following general function:

$$F_o = f(d)(\lambda)(w-w_o) \qquad \text{- - - - - (5)}$$

in which
where: d = diameter of particle

λ = void ratio

w = ~~specific gravity~~ weight per unit volume of sand

w_o = specific gravity ~~of fluid~~ weight per unit volume of water

It is almost impossible to derive constants or coefficients for this formula.

The following are experimental formulas:

B. du Boy's computation:

The sand particles on a river bed under stable conditions interlock one another and do not permit individual motion. From the above statement du Boy concluded that the stability of a stable river bed is determined by the thickness of the sand layer which resists tractive force. If the flow is uniform and steady, the tractive force on a unit area is $F = W_o HI$, The frictional resistance of a sand layer having thickness d is $R = f(w-w)\ (1-\lambda)\ (1.1.d)$, in which λ is the void ratio and f is a coefficient of friction.

At the limitation of stability of a bed

$F = F_o$ and $F_o = R$, so that

$$d = \frac{W_o HI}{f(w-w)(1-\lambda)} = \mu HI \text{ ----------(6)}$$

in which d and H should be expressed in common units and $\mu = 1.5 \sim 2.0$

In the case when the diameter of the sand particle d_o is less than thickness of the sand layer d given by Eq. (6), he assumed that n layers of d_o ($nd_o = d$) move together and the formula becomes

$$F_o = W_o HI = (w - w_o)\ (1-\lambda).nd_o \text{ ---------(6}^1\text{).}$$

This concept of the motion of several layers disagrees with actual conditions and also neglects to consider the shape, size and distribution of particles. Hence this concept is risky to apply in the field. Nevertheless it is worthy of attention as one of the first methods of computation based on the tractive force theory.

C. Schoklitsch's experimental formula:

By using depth of water less than 8 cm, Schoklitsch found a formula for critical tractive force F_o, for the begin-

ning of motion of sand particles.

$$F_o = \sqrt{0.385\, w(w - w_o)\eta \overline{\nabla}} = \sqrt{0.201\, w(w-w_o)\eta\, (2a)^3} \quad -- (7)$$

where: $\overline{\nabla}$ = volume of sand particle (m^3)

$2a$ = mean diameter of particle (m)

η = shape coefficient; sphere = 1, sand = 1.15 - 1.35, thin debris of rock = 4.4, debris of rock = 3.1.

If the volume of sand is $\overline{\nabla}$, and the actual volume of sand particles neglecting voids is $\overline{\nabla}_s$, then

$$F_o = \sqrt{0.385\, w(w-w_o)\eta\overline{\nabla}/\left\{1 + \left[10.5\left(\frac{\overline{\nabla}}{\overline{\nabla}_s} - 1\right)\right]^{\frac{1}{4}}\right\}} \quad -- \quad (7')$$

Eq. 7 and 7' define tractive force as F_o when a particle starts moving. Since the sand particles are interlocked with one another in natural rivers, these formulas do not seem adequate to apply in the field. But these formulas are worthy of an examination as an experimental proof of the tractive force theory.

D. Krey's experimental formula:

He assumed tractive force as F_o at the time when all the particles start moving, and it is difficult to evaluate the number of individual particles which are moving. Under these conditions he proposed that the frictional resistance $R = f(w - w_o)\pi d^3/6$ equals the tractive force $F_o \pi d^2/4 = w_o HI \pi d^2/4$ in each particle. Assuming sand particles as spheres with diameter, d, he derived the following formula:

$$d = \zeta \frac{w_o}{w - w_o} HI, \quad \zeta = \frac{3}{2f} \quad -- \quad (8)$$

After many experiments he proposed $\zeta = 13$ and thus Eq. 8 becomes

$$d = 13 \frac{W_o}{w - W_o} HI, \quad \text{---------- (8')}$$

If $w = 2.6 \sim 2.7$, $d \approx 8 HI$, in which H and d have same units

There is no adequate measure for river beds having nonuniform material. However, as d in Eqs. 8 and 8', is used, the average value of the mean diameter d_m and the median diameter d'_m obtained by plotting the size-distribution as Fig. 1 and computing from Eq. 9, Eqs. 8 and 8' may be

Fig. 1

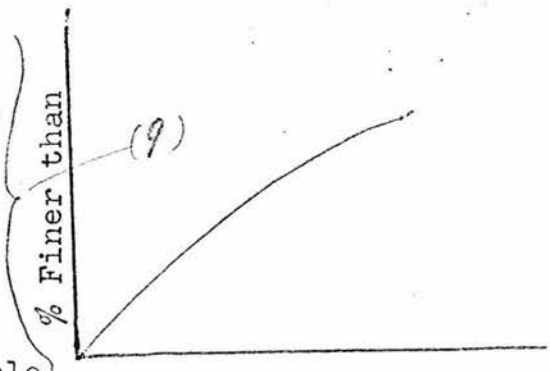

$$A_A = \sum_{p=50}^{100} d\Delta P; \quad A_B = \sum_{p=0}^{50} d\Delta P$$

$$A = A_A + A_B = \sum_{p=0}^{100} d\Delta P; \quad P = \sum_{P=0}^{100} \Delta P$$

$$d_m = A/P \; ; \quad d'_m = (P = 50\%) \text{ Size of particle}$$

Krey's experimental formula has an inadequate coefficient for the case of non-homogeneous particles, but it is still convenient to apply this formula in the field. This formula has been used as a guide in the present study.

E. Kramer's experimental formula:

Kramer used a $30^{cm} \times 80.7^{cm} \times 17^{m}$ flume with sand of different diameters and proved the general conclusions, stated in A, by experiment. At the same time, by using the result of his experiment and data of other authorities in Europe, he derived an experimental formula corresponding to the theoretical formula given in Eq 5.

Kramer applied the method which Himmel used for the determination of the characteristics of concrete aggregates

and also applied mean diameter $d_m = A/P$ and the coefficient of homogeneiety $M = A_B/A_A$ from Eq 9. His formula expresses the relationship between the size of particle, its distribution and the void ratio, and is written as follows:

$$F_o = \frac{100}{6} \frac{d_m (w - w_o)}{M} \quad \text{- - - - - - - - - (10)}$$

where: F_o = critical tractive force (g^r/m^2) = 10^6 HI,

H = depth of flow (m),

I = slope of water surface = slope of bed,

d = mean sand diameter (mm), and

and M = coefficient of homogeneiety ($M = A_B/A_A$)

In his experiments, Kramer fixed the bed slope and kept the flow uniform and steady then he increased the discharge. He assumed the time sand particles start moving and when little ripples were formed as the condition for bed stability and computed values of F_o from the depth of water and the slope of the bed.

Indri made rigrous experiments on sands of many sizes, and using his data and the experimental work of Meyer-Peter and Gilbert, he revised Eq.10 as follows:

$$\left.\begin{array}{ll} d_m < 1 \text{ mm} & F_o = 13.3\, d_m \quad \frac{w-w_o}{M} + 12.16 \\ d_m > 1 \text{ mm} & F_o = 54.85\, d_m \quad \frac{w-w_o}{M} - 78.48 \end{array}\right\} \quad \text{- - - - - (11)}$$

Eqs.10 and 11 are dimensionally correct. Since these formulas contain all the necessary terms, they can be applied to river models. Moreover, the formulas are in a simple form

and each term can be easily and accurately measured. Although, these formulas are inadequate in the determination of coefficients, they are more reliable when compared with other formulas.

(7) Model Tests Concerning Scour

As stated before, the scour in an alluvial river bed is largely related with velocity, discharge and the characteristics of sand. It is difficult ~~in experiments~~ to establish complete similarity between models and prototypes. Accordingly, it is difficult to predict quantitatively the prototype conditions from model tests. Moreover, for a qualitative prediction of the actual conditions it is necessary to select sand with the proper size sand for the model bed, such that scour begins to occurs ~~at the same rate~~ under corresponding conditions. It is almost impossible to reduce the size of sand particle to the model-prototype ratio. If by any chance, it is possible, as a result of difference in interlocking ability, the mechanics of scour will change and model-prototype comparison will be difficult.

In general:

	Length	Width	Depth or Head	Slope	Velocity
Model	l^{χ}	B^{χ}	H^{χ}	I^{χ}	V^{χ}
Prototype	$l=ml^{\chi}$	$B=mB^{\chi}$	$H=nH^{\chi}$	$I=\frac{n}{m}I^{\chi}$	V

	Discharge	Coeff. of Velocity	Critical Tractive Force	Sand Diameter
Model	Q^{χ}	C^{χ}	F_o^{χ}	d^{χ}
Prototype	Q	C	F_o	$d=ed^{\chi}$

If we let m > e such that the ratio of reduction of particle decreases, and if m > n so that the model ratio for depth decreases, and we let the slope be larger than the actual slope then the scour phenomena in the model will be similar to that in an actual river. According to the limit of the experimental equipment, it is necessary to reduce the value of m as much as possible. The value of n can be computed from Eqs. 3-11.

For example: Assume S and w are constants both in the model and prototype. Using Eq. 8 (Krey's)

$$\frac{d}{d'} = \frac{HI}{H'I'} \; ; \; \therefore \; e = \frac{n^2}{m} \quad - - - - - - - - (12)$$

If m and e are given, n can be determined. In natural rivers the flow is turbulent and ~~tranquil~~ subcritical instead of ~~rapid~~ supercritical. A similar kind of flow pattern is desireable for the model tests.

Krey proposed a formula relating the slope, the diameter of sand particles and the velocity of flow for a model, as follows:

$$\frac{d'}{\delta H'} < \frac{I'}{\left(\frac{C'^2}{g'}\right)} < \frac{g'}{C'^2} \; ; \quad V' < \sqrt{g' H'} \quad - - - - - - (13)$$

Therefore for the determination of the model ratio, use eq. 13 as a limiting condition and determine the values of e, m and n which will satisfy Eq. 12.

Vogel proposed that the terms which should be considered for the determination of the model ratio are in the following order of importance:

a. Within the range in which the measurement of depth is possible, for turbulent and ~~tranquil~~ subcritical flow conditions, determine the values of m and n. They

should be as large as possible and with little difference in magnitude between them. For the above reasons models should fit the relationship.

$$\frac{0.020}{H^2} < V^2 < \sqrt{gH^2} \quad \text{(Ft - sec. system)}$$

b. Obtain the critical tractive force, F_o, by using sand of river bed material size or by applying Eq.10.

c. Using the river bed slope and F_o obtained from b, determine the depth of flow of river at the time when the bed begins to scour.

d. By method b, determine the critical tractive force F_o^2 for the bed material of the model.

e. From the model ratio for depth and the results obtained in c, the depth of flow in the model at the time when scour starts can be determined. Knowing depth of flow and the critical tractive force, necessary the slope of model bed I' can be determined.

f. Tilt the model such that slope becomes I^2. Therefore, the model ratio for slope $i = I/I^2$ is different from the one determined from the values of n and m.

For practical applications, the author described the method to determine chose the model ratio, m, n and e (Vogel added i), for model tests on scour. It is important to determine adequate model ratios for each hydraulic quantity, such as discharge, velocity, time and amount of scour etc., for the purpose of getting complete

hydraulic similarity between the model and prototype.

In general, the Froude law of similarity is used in determining the model ratio for channels in which the hydraulic phenomenon is mainly controlled by gravitational forces, such as channels having large hydraulic radius. But when friction of channel wall is evident the Reynold's law of similarity has to be considered along with the Froude law of similarity. It is impossible to use these two laws simultaneously; hence, models should be designed such that wall friction of model is equal to that of the actual structure. There is no complete study on the change of the coefficient of friction resulting from the model ratio. This fact causes difficulties in practical application.

At the present time, the model ratio is determined by using the mean velocity formula. For example, Vogel determined the model ratio by using Manning's formula

$$\therefore \frac{Q}{Q'} = m^{1/2}\, n^{13/6} \qquad \text{- - - - - - - - -} \qquad (14)$$

In deriving this formula, Vogel applied the fact that the coefficient of roughness of a cement mortar model ($m < \frac{1}{1000}$), having a sand bed ($\frac{1}{1000} < m < \frac{1}{500}$) and of natural rivers are approximately equal. This approach is worthy of notice.

In the case of an alluvial bed where the gravitational force can be considered as the main effective force, the Froude law of similarity can be applied. However, when the friction on the river bed has an evident effect on scour from

natural river beds, the model ratio is generally determined by using a mean velocity formula. For example Okubo derived the following equation by using Chezy's formula:

$$\frac{Q}{Q'} = m(n^2 e)^{\frac{1}{2-2\beta}}; \quad \frac{V}{V'} = m^{-\frac{1}{2-2\beta}} n^{\frac{1/\beta}{1-\beta}} \quad \text{----(15)}$$

$$i = \frac{n}{m}$$

According to Winkel's study, the velocity coefficients can be found as follows:

$$C = A(V R^{\beta} K)^{\beta}; \quad C' = A(V' R'^{\beta} K)^{\beta}; \quad \text{where } K = \frac{1.2}{10^{\rho_K}}$$

These expressions can be applied only when K and the coefficients A and β are the same for the model and prototype. In natural rivers $\beta = 1/8$, $A \approx 42.1$, then Eq.15 becomes

$$\frac{Q}{Q'} = m(n^2 e)^{4/7} \frac{V}{V'} = m^{-4/7} n^{9/7}$$

A smooth model surface is beneficial in obtaining hydraulic similarity between model and prototype. This purpose is accomplished by placing different materials having less specific gravity w' than that of sand in the model, thus reducing both the value of e and the difference between m and n.

In this case, an expression can be obtained, by using Eq.8. instead of Eq.15, as follows:

$$\frac{Q}{Q'} = m\left\{n^2 e\,(w-w_o)/(w'-w_o)\right\}^{\frac{1}{2-2\beta}} \quad \text{------(15')}$$

$\frac{V}{V'}$ is the same as for Eq.15.

The methods stated thus far are mainly for the experiments on general scour and those on the movement of sand particles, caused by improvements on the river channel.

It is doubtful, however, whether the quantitative and qualitative conclusions derived from the above theories are applicable to local scour caused by piers. Even in rivers with fixed beds, the problem of backwater due to piers and the resulting dynamic pressure are still far from solved. Accordingly, it seems difficult to find a dependable law of similarity for experiments on local scour caused by piers.

The experimental results discussed in this paper are mainly qualitative and it is regretable that no adequate measure is available for applying these experimental results to natural rivers.

III EFFECT OF PIER SHAPE ON SCOUR

(8) General

The most effective and economical measure for the stability of piers is to form the piers of shapes which give the least resistance to flow and cause no evident backwater or scour. However, pier shape is limited from the viewpoint of structural stability and construction.

Durand-Claye (1873) ran a series of experiments on the effect of pier shape on scour. Engels (1894) continued Durand-Claye's work. Later, Rehbock (1921), Winkel (1929) and Keutner (1932) did some more experimental work on scour and gave qualitative conclusions. Because of the impossiblity of obtaining a complete law of similarity, they used small models, and neglected to take the bed material into consideration.

Hence, it is difficult to attribute the qualitative differences of scour in their experiments to the pier shape. It is also difficult to apply their findings to an actual case in the field.

For the study of scour caused by two lenticular piers (with sharp noses) of lenght 20^m and width 4^m placed 14^m apart in a 50^m wide river having a depth of 5^m and a discharge of 1000 m^3/sec., Kurt Schwarz (1924-1925) used models having a model ratio of 1:100 and three sizes of bed material.

1. Diameter of individual particles less than 1.5 mm, of which 67% are less than 0.4 mm.
2. Diameter of individual particles less than 1.0 mm, of which 78% are less than 0.4 mm.

3. Diameter of individual particles less than 0.5 mm, of which 95% are less than 0.4 mm.

By setting the time of run from 3 minutes to 9.6 hours for 23 runs, he found that considerable difference in scour pattern development for each time interval by changing the bed material. His results are shown in Fig. 2. This fact is noticeable in a study of the law of similarity on the problem of scour caused by piers

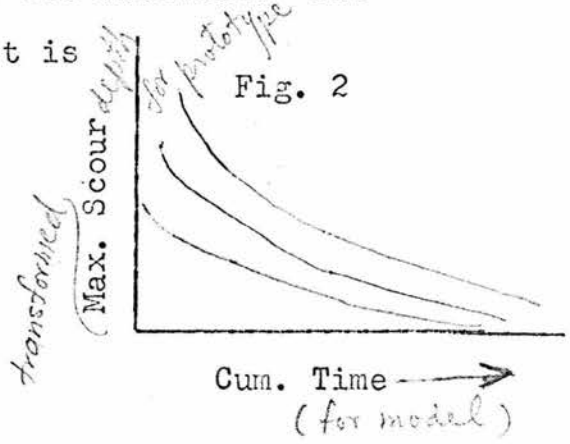

Fig. 2

This paper presents the experimental technique and results on to evaluate the effect of pier shape on scour.

(9) The Purpose of the Study and the Experimental Technique

A. Purpose of study:

For investigating the effect of pier shape on scour, the author made a preliminary experiment on critical tractive force on a river bed without piers, thus verifying the contention of Kuetner and Kramer that a river bed has a constant critical tractive force for each different size material. Models of several shapes were then inserted at the center of flow for 20 minutes under conditions of critical tractive force determined previously. In these experiments, the author investigated the effect of pier shape on scour and also observed the flow pattern around the piers to study the mechanics of scour.

Using the law of similarity for models, the author tried to derive quantitative relationships from qualitative experimental

results but omitted them from the discussion in this paper.

B. Equipment for experiments:

A circulating flume 20m x 1.82m x 0.455m with a maximum bed slope of 1/25, as shown in Figs. 3-5 (p.36) was used for running the tests. The maximum discharge possible through the circulating system was 55 l/sec. Water is pumped to a tank of $2.70m^3$ capacity and is kept at a constant height by a spillway, then allowed to flow to the upstream end of the flume through a pipe. The discharge is controlled by a valve on the pipe and is measured by a sharp edged Bazin rectangular weir connected with the downstream end of the experimental flume. The steel tail gate was used in adjusting the depth of flow. The tail gate was operated very accurately, thus the required depth was kept constant for each run. easily obtained. Thick circular paper of 1cm diameter was used to measure the surface velocity of flow.

C. Pier models:

In order to obtain applicable data to the field For the purpose of comparison with available field-~~data~~, wooden models of existing pier shapes were made. These constructed with the rectangular box and models were of dimensions 30^{cm} x 15^{cm} x 45^{cm} with nose and tail as shown in Fig. 7 and Table 3. Fig. 8 is a photograph of the nose and tail which were used in the experiments. For the purpose of studying the effect of pier length, pier models of length l_1 = 5, 10 ... 60^{cm} were constructed. Circular pier models of 15^{cm} diameter and 45^{cm} hight were also constructed. Acutally, from the point of beauty and stress, the cross-section of the lower part of pier should be larger than the upper part. From the viewpoint of scour, it is beneficial

for the nose of pier to have a slope of 1:2.5 instead of being vertical, but in order to simplify the comparative study on the scour phenomenon piers with a constant crosssection throughout were used.

D. Sand used for experiments:

Sand passing No. 8 sieve was filled to a depth of 10cm in the middle 10m of the test flume. Water was slowly added until the sand was covered with water, and the bed was screeded to the required slope. The water was drained from the flume in order to avoid the effect of water, before scour measurements were made. Table 4 is a sieve analysis of the bed material collected from the bed at 5 different locations.

E. Preliminary experiment to determine critical conditions:

-Determination of critical conditions. The critical tractive force F_o for the sand analysed in Table 4 was computed by Kramer's experimental formula (10) and Indri's experimental formula (11), which were assumed most reliable. The computed values of mean F_o were 64.15 g/m^2 and 63.35 gr/m^2 from (10) and (11) respectively. In order to ascertain these values experimentally, first, the bed slope was set as 1/800. By controlling the tail gate, water surface paralled to bed surface, to obtain uniform steady flow was established. Under these conditions, the discharge was increased untill the bed material started moving completely. The formation of ripples was recognized as the limit of bed stability. At the critical condition the discharge, the depth of flow and the surface velocity were carefully measured. Fig. 9 is a surface velocity distribution

curve measured at the critical condition. There was no evident ripple charge 30 minutes after critical conditions were reached. But, as a result of gradual irregularity in the bed surface, relatively high ripples, about 2~3 0/0 of the flow depth, were observed after 60 minutes.

The above experiment was repeated and flow depths, at critical condition, of 5.17^{cm}, 5.20^{cm}, and 5.19^{cm} (mean 5.19^{cm}) were measured. Then

$$F_0 = 10^6 \times 0.0519 \times \frac{1}{800} = 64.88 \ gr/m^2$$

For a second experiment, a bed slope of 1/600 was set and flow depths, at critical conditions of 3.94^{cm}, 3.91^{cm} and 3.90^{cm} (mean 3.92^{cm}) were obtainted. Then

$$F_0 = 10^6 \times 0.0392 \times \frac{1}{600} = 65.33^{gr/m^2}$$

A slight difference between these values is recognizable. However, owing to the difficulty in the determination of critical conditions, this difference is considered as experimental error. Thus it has been shown that the F_0 is constant for each size of bed material. Based on the above mentioned conclusion, the critical tractive force of the bed has been decided assumed as $F_0 = 65^{gr/m^2}$. This value has been used in Table 5 as critical conditions for the scour experiments. In Table 5 shows the * are measured values. The wall of the flume was painted before the testing program, hence the wall effect was very slight, as shown in Fig. 9. Moreover, the depth of water was used as the hydraulic radius for computing the velocity coefficient in Table 5.

F, Experimental technique:

For investigating the effect of the shape of nose and

tail on scour, a rectangular box of $l_1 = 30^{cm}$ and different shapes of nose and tails, as described before were used. A pier model was placed at the center of the flume and the water was allowed to flow, at critical conditions (as Table 5), for 20 minutes. Accurate measurements of water surface around the pier were made during the experiment. After the flow was stopped, scour depths were measured by means of a point gage. For investigating the effect of pier length, rectangular models of lenght $l_1 = 0,5,10,....60^{cm}$ with circular noses and tails arranged in parallel with flow were used. Two circular pier models of 15^{cm} diameter were also investigated. Table 6 is measured terms.

(10) Effect of Pier Nose Shape

Minard (1856) proposed that the scour at the pier nose is always maximum and effects the stability of the pier itself. Later, Rehbock and Keutner stated that the scour around piers is evidently affected by the shape of the pier nose and it is advantageous for reducing the scour to sharpen the pier nose. From the author's test, series A_1, A_2 and B, this fact can be recognized. As seen in Fig. 10 the scour is symmetrical on each side of the pier parallel to flow with maximum scour being found along the pier nose. In the following, the results of the tests are shown with the notations defined in Fig. 11.

A. ~~The results of test~~ Series A_1 and A_2 ~~are as shown in Fig. 11 and Table 7~~ shows the measured values of the scour width and depth around the nose.

The depth and width of scour are considered affected by the angle 2α of nose of pier. This relationship is shown in Figs. 12 and 13. If the angle between the line tangent to the nose at the transition point F to the side of the pier and the center line of flow is β, the relationship of β with the scour depth and width is as shown in Fig. 14. It is beneficial for reducing scour to enlarge the ratio of length

of nose to half of its width $2\ell_2/b$. The $2\ell_2/b$ ratio is limited by economy and structural and construction difficulties. Fig. 15 is a relationship between $2\ell_2/b$, scour depth, scour width and the horizontal cross-section of the scour hole. In Figs. 12 - 15, the continuous lines are for an arc type nose and the dotted lines are for a straight type nose. The following salient points from these figures are worthy of notice:

i) The relationship between the angle of nose of pier and the scour width K_o and k_s is shown in Fig. 12. It is seen that the smallar the angle the smaller the scour width. This decrease in scour width with a decrease in angle is obvious for angles less than 40° for an arc type nose and 30° for a straight type nose. But for a straight type nose, there is a little effect of nose angle for angles less than 20°. From Figs. 14 and 15, an increases in k_o and k_s can be observed with a decrease in ℓ_2 for an arc type nose ($\alpha = 90°$). This is due to an increase in θ. For the same value of α, k_o and K_s are larger for the arc type than the straight type nose. These facts can be observed from Fig. 15. For two arc type pier noses, k_s is found to be inversely proportional to $2\ell_2/b$. The relationship stated above are important for the determination of pier shape and for providing protection.

ii) Smoothness of the transition point F seems important in decreasing k_f but, it is seen from Fig. 14 that k_f is only slightly affected by the angle β for an arc type pier nose and there is measureable effect for the straight type pier nose only when β is less than 45°.

iii) For an arc type nose, as seen from Fig. 13 the scour depth at the top of the nose, t_s, and that at the transition point F, t_f, decrease considerably when α is less than 60° and 40° respectively. Moreover, for the case where α is larger than 50° t_s is larger than t_f ($t_s > t_f$) and for α less than 50° it is vica versa, i.e., $t_f > t_s$. The maximum scour occurs along the side of the nose F. When α is small it moves towards f, and when α becomes large it moves towards the tip of the nose. The straight type nose has the same tendency as the arc type nose except $\alpha = 60^\circ$ is the demarcation point between t_s and t_f. $t_{max} \approx t_f$ ($\alpha < 60$) $\approx t_s$ ($\alpha > 60^\circ$). Values of t_s and t_f for the straight type nose are larger than those for the arc type nose having the same angle α. One disadvantage of the straight type nose is its inability to appreciably decrease the scour depth t_f by decreasing the angle of nose α. There is no difference in t_f for a straight type and an arc type nose for the same value of

of 2 2/D but t_s for a straight type is less than that for an arc type, as shown in Fig. 15.

iv) The pile-up of sediment near the tail of a pier has the following approximate variation:

$h'_s = 1.0 \sim 2.5^{cm}$

$h_u = 2.0 \sim 3.5^{cm}$

a'_f $af' = 15 \sim 20^{cm}$

a'_u $a_u' = 85 \sim 110^{cm}$

The pile-up has no evident effect on the stability of the pier itself. The size of the pile-up is scarcely affected by the shape of nose and especially for the two arc type nose, the above values are almost constant. As seen from the experimental procedure, the results show only the effect of pier shap on scour. Hence these results give a qualitative measure for pier shape design.

B. Comparison with Keutner's experiment:

Keutner used a flume of 0.65^m width with a layer of sand 0.2^m thick covering the bed and established a depth of time varying run ~~varied~~ between 150 minutes and 480 minutes. Zinc boxes of 12^{cm} width 25^{cm} length, and 50^{cm} hight with 8 kinds of arc type noses and tails were used as models. Fig. 16 is a plot of the experimental results for a model with two arc type noses and a semicircular tail. For this test series, $k_o \cong k_f$ when $\theta = 90^\circ \sim 31.3^\circ$, and $k_o \cong k_s$ when $\theta = 14.5^\circ$. Maximum scour t max, occurred at the top of the nose when $\theta = 90^\circ$ then

t_{max}

moved to F with a decrease in the nose angle θ and occurred again at the tip of the nose when $\theta = 14.5^{\circ}$.

From the curve, Keutner proposed $\theta = 38.3^{\circ}$ as the ideal pier nose angle from the standpoint of scour protection. The author, considering the practical application, used θ larger than $33^{\circ}.24'$ for the two arc type nose and $16^{\circ}42'$ for the straight type nose. The author doubted Keutner's experimental conclusion that k_o and t_{max} were considerably reduced when $\theta = 38^{\circ}.30'$ and that maximum scour occurred at the top of the nose. When $\theta = 14.5^{\circ}$ Keutner attributed these conclusions to the sudden change in scour mechanism caused by a change in the flow phenomenon. The experiments performed by the author did not verify Keutner's findings. Keutner neglected to consider bed material as a variable and thus erosion of the bed might have occured even if before the piers were not inserted. This may be the reason for the different findings of Keutner and the author.

C. Series B: Table 8 and Fig 17.

Comparing the result of series B, Table 8 and Fig. 17, with series A', it is seen that variations due to nose shape are almost similar. Moreover, series A and B were run under different critical flow conditions, (a) and (b) respectively.

Judging from these conclusions, the qualitative relationship for pier shape obtained in these experiments are applicable for natural river of different size bed material and under different flow conditions.

(11) The Effect of Pier Tail Shape

According to Engels the shape of a pier tail does not affect scour around a pier nose. This statement was verified by Keutner. Slight scour was observed at the pier tail inspite of pile-up of sand at the rear part of pier. Keutner, judging from this fact, proved that there is some effect of tail shape on the river bed, However, scour and pile-up of sand at the pier tail do not effect the pier stability itself. Scour at the pier tail is assumed to be controlled by the factor $\tan^{-1}\left(\frac{2l_2}{b}\right)$, where l_2 is length of tail (Fig. 11).

From the results of series C_1 and C_2, Table 9, the author has shown that the shape of the pier tail does not effect scour around the pier nose. In these series, the pile-up (hights were less than 3 m) of sand behind the piers were measured but scour did not occur.

By decreasing the angle of tail $2\partial_1$, the following phenomena were observed:

a. height of pipe-up l_s and h_u increased ;
b. width of pile-up a'_u and distances a_u decreased ; and
c. Scour depth t_f and distances a_c, a_f, a_v and a_h did not change.

If the flow around a pier is tranquil, backwater and flow resistance on pier are considerably affected by vertical eddies along the pier tail. Rehbock proved this fact and proposed piers with stream-lined tails, so that eddies are kept to minimum. As stated before, the sharper the pier nose the less the nose scour of pier. Despite the effect of pier tail eddies on the sand pile-up, the nose scour is entirely unrelated to these eddies.

In the present paper,

A pier having a sharp nose and tail is suggested as the ideal shape, because a sharp nose and tail reduce the scour, decrease the backwater and the resistance to flow.

(12) The Effect of Pier Length

Pier models, with a semicircular nose and tail of constant width 15 cm and length varying from 5 cm ~ 60 cm were used as models for series E. The data for scour at the pier nose is shown in table 10 and Fig. 18. The followings are the salient conclusions worth mentioning:

1. The scour width K_o^k and k_s at the pier are not related to pier lenght.
2. When l 1/b is less than 1, the scour width k_f is fairly constant but there is a slight increase in k_f as l 1/b exceeds 1. This is because of the deflection of separated effects of inclined flow at the pier nose. For small l 1/b, the separated flow will straighten out near F tend to return to the pier but, for large l 1/b, the deflection of separated inclined flow will continue further towards the flume wall.
3. Scour depth t_s and t_f are almost unrelated to pier length. Only when l 1/b is very small, these values increase slightly. On the contrary, t_f decreases considerably with an increase of l 1/b, moreover, when l 1/b is larger than 3.0, piling-up of sand will occur. This is because t_f^1 is directly affected by scour at the nose when l 1/b is small, also when l 1/b increases, sand piles-up at the tail due to the effect of vertical eddies along the pier.

4. It is not necessary to consider sand pile-up at the pier tail in connection with the stability of the pier. However, the variation of size of pile-up with respect the ℓ 1/b is as follow (refer to Fig. 11)

h_s = -0.4cm → ≠ 1.5 cm → ≠ 0.7 cm,

h_u = ≠1.5 → ≠ 2.5 → ≠ 1.1 cm,

a_s = 1.3 → 4.1 cm, a_u = 1.5 → 4.5 cm,

a_v = - 20 → ≠47 cm, a_h = ≠29 → -10 cm,

$a_{f'}$ = 15 → 11 cm, and $a_{u'}$ = 110 → >0 cu.

The hight of pile-up increases for ℓ 1/b between o and 1.33 and then decreases with higher ℓ 1/b values.

a_s, a_u and a_v increase as ℓ 1/b increases, on the contrary, a_h, $a_{f'}$ and $a_{u'}$ decreases except $a_{u'}$ is almost constant for ℓ 1/b between o and 1.33.

Judging from the above conclusions, it can be shown that the length of a pier has no affect on the nose scour which is the main controlling factor for pier stability.

(13) Two Circular Piers

A. General

Data for two circular piers is very important at the present time, yet only a few experiments performed by Nagler and Timnoff are available for two circular piers. Timnoff made his experiments on a new circular pier which is to be constructed near an old bridge pier. His conclusions are:

1. The stability of a pier is mainly controlled by scour at the pier nose. If the old pier has a deep foundation it is advantageous to construct the new pier downstream and as close as possible to the old one. On the other hand, it is better to construct the new pier upstream if the old pier had a shallow foundation. A new pier thus located will protect the old one from excessive scour.
2. In case the spacing of the piers are not the same, the new pier should be constructed upstream of the old one if its spacing is larger and down stream if it is smaller. Here again it is advantageous to locate the pier as close as possible to the old one.

Considering the above findings it is suggested that the two piers be put so close to each other that the pile-up at the tail of the front pier may fill up the scour at the rear pier, thus avoiding the disturbance of the river bed. Series F was run to investigate the relationship between scour and the spacing of two circular piers.

B. Series F

The result of series F for two circular pier models of 15 cm diameter are shown in Table 11 and Figs. 19 and 20. The important conclusions derived from the series are as follow:

1. Scour widths k_o and k_s at the point S are independent of the spacing of piers, l_1, while k_f slightly increases with increase in l_1. Thus it seems that the values k_o, k_s and k_f may be reasonably considered as

related only ~~with~~ to the front pier. Comparing Table 11 with Table 7, it is found that the two circular piers had a similar scour pattern to the wall type pier.

2. Scour depths t_s and t_f are independent of the spacing l, but a relatively large variation of $t_{f'}$ with respect to l, was observed. As seen from Fig. 20, $t_{f'}$ decreases for values of $l_{1/b}$ between ~~1.00~~ and ~~2.00~~ 1.67, but a further increase in the $l_{1/b}$ ratio does not affect the values of $t_{f'}$. In general, when the $l_{1/b}$ value is near 1, the pile-up of sand caused by the front pier is less than the scour caused by the rear pier, hence $t_{f'}$ is relatively large. As $l_{1/b}$ increases, the piling-up of sand is evident and thus $t_{f'}$ decreases. For a larger value of $l_{1/b}$ than a certain values of $l_{1/b}$, these effects are approximately constant and $t_{f'}$ does not change much. The same reasons may be applied to the scour t_2 at the rear pier.
Of course, for extremely large values of $l_{1/b}$, $t_{f'}$ and t_2 will be the same as t_f and t_s respectively.

3. When $l_{1/b} \leq 2.67$, there is only a little pile-up of sand near the point Am and considerable scour will occur on the entire bed surface around the piers. A sudden increase in scour depth downstream of the line Am, $k_2 = A_m K_2 K_{f'}$ $k_{f'}$ is the effect of the scour around the rear pier nose. As seen from Fig. 20 the values of Am, k_2 a_m

and k_f', which are affected by the scour and pile-up caused by the front pier, have a measureable change as the values of $\ell_{1/b}$ change, and these values approach k_o, k_s and k_f as the values of $\ell_{1/b}$ approach infinity.

4. The variations of t_1 and t_2 are similar to that of t_f' but only t_2 has the same reason as t_f', previously stated in 2. It is appropriate to explain the variation of t_1 as follows:

When $\ell_{1/b}$ is approximately 1, t_1 is affected by scour at the rear pier. Hence the value of t_1 is large increases. Since this effect decreases with an increase in $\ell_{1/b}$, t_1 also decreases to a certain extent. However, for larger vaules of $\ell_{1/b}$ than a certain value, When this condition is established, a further increase in $\ell_{1/b}$ does not affect the value of t_1.

5. The pile-up of sand observed behind rear pier is as follows:

h_s'

$h_s' = 1.9 \rightarrow 2.3$ cm

$h_u = 1.9 \rightarrow 2.7$ cm

$a_u' = 100 \rightarrow 70$ cm

h_s

$a_u \approx 1.5$ cm

$a_s \approx 1.7$ cm

h_s' and h_u increased slightly as $\ell_{1/b}$ increased from 1 to 2, and then were approximately constant. a_u' was constant when $\ell_{1/b}$ increased from 1 to 2 but a slight decreased was observed with a further increase

in l_1/b. The pile-up along the line AnAv was evident only when $l_1/b < 2$. Values of a_v between 6cm and 7 cm and a_h between 10 cm and 14 cm were measured. In general, two circular piers are similar to the wall type pier. However, the disadvantage of the two circular piers is the relatively large scour hole between the two piers. This effect is balanced by filling and scouring caused by the front and rear piers respectively when the value of l_1/b is near 2.

14. Effect of Flow Time

Scour increases with time to a certain extent until equilibrium is established, then only very slight scour occurs. In series D, 30 cm rectangular models with a semicircular nose and tail were used at the critical flow condition (a). The results of this series of runs are shown in Table 12 and Fig. 22 (Refer to Fig. 11). Scour was evident for the first 5 minutes but the change in scour depth was very slow after 20 minutes. According to Keutner's experimental study, and increase in scour is more evident for large values of 2α. Fig. 22 is a plot for $2\alpha = 180^\circ$, so that, for small values of 2α, the time required for reaching equilibrium is less than that shown in Fig. 22. The above mentioned reasoning was followed by the author in choosing 20 minutes as the run time for his experiments.

15. Conclusions

1. A river bed has a constant critical tractive force

Fo and its numerical value can be obtained from Kramer's formula. If the tractive force is less than the critical Fo, the effects of depth, H, and slope, I, on the scour phenomena are almost similar. The scour depth and scour width decrease with a decrease in flow depth and a increase in slope if the flow is at the critical condition.

2. Scour occurs within a relatively short period. The increment of scour is less with increasing time.

3. The scour at the pier nose is mainly affected by the nose shape and is independent of the length of pier and the tail shape. Scour decreases by sharpening the nose, and the scour pattern is measureably affected by the angle of nose 2α. The scour patterns for the arc type and the straight type pier noses are quite different. However, it is difficult to conclude which type nose is superior.

4. The results of these experiments can be applied to the practical design of bridge piers in the field. However, economy, structural stress, ease in construction and beauty are also factors that should be considered in the ~~ultimate~~ design of the bridge piers. The author proposes using a nose angle $\alpha = 35 \sim 40^\circ$ for the circular type nose and $\alpha = 20^\circ \sim 30^\circ$ for the straight type nose. He also recommends using a tail angle 1.5 ~ 2.0 times as much as that of the nose.

5. Serious scour occurs between the two piers when two circular piers are used, hence it is recommended that this type of arrangement not be used. In case of economic reasons dictate using this type of pier, it is desirable that the spacing between piers be approximately twice the diameter of the piers.

16. Additional Remarks

A. The effect of pier arrangement on scour.

In regards bridge maintenance and river regulation, the following factors should be considered before constructing a bridge.

1. The bridge should be constructed on a straight reach of the river.
2. Skew bridges should be avoided and the piers should be paralled to flow.

But these requirements are difficult to satisfy due to economical and geographical limitations. In natural rivers the flow direction is not always parallel to the piers, especially, during flood flows, although it is difficult to judge its direction, it is usually assumed to be parallel to the banks of rivers for determining the direction of piers.

For investigation the relationship between diagonal flow and scour, the author is running ran some tests (Series G) on 30 cm rectangular models with a circular nose and tail. The tests were are being run under critical flow condition (a) and the angle between the flow and the pier varied varys from 5 °to 40°.

Keutner used models having a two arcs type ($2\theta = 101^{\circ}$) noses, a And a semicircular tail and used 150 minutes as the flow time. His results are as follow:

When the angle of skew to flow is less than 5.5° the scour pattern is the same as for $\theta = 0^{\circ}$. Hence it is desirable to construct piers with angle of skew to flow less than 5.5°. Moreover, when θ is less, the pier will callapse toward the nose in case of scour failure, but when θ is more than 21.5° the pier will fall perpendicular to the pier axis towards the upstream. Thus it is necessary

to protect the river bed both at the nose and the upstream side of a pier.

B. The mechanism of scour.

Keutner, based on his experimental study, explained the mechanism of scour as follows:

> Due to the pile-up of water at the pier, a lateral slope will be formed along the line perpendicular to the pier axis. Edies are formed as a result of this lateral slope and these eddies along with the bottom flow, scour the bed. The lateral slope is mainly controlled by the nose shape. In front of the nose the water surface forms a reverse slope to the flow and considerable scour occurs. Most of the sand scoured out at the pier nose will pile-up near the tail due to the vertical eddies along the tail.

C. Protection of scour.

A reasonable pier arrangement, an adequate cross section and a deep foundation are important in decreasing scour and increasing pier stability. Armorplating, riprap, protective mats and masonary block are the most effective methods for improving pier stability.

The qualitative result of these experiments are also a reasonable guide for scour protection in the field. Engels proposed using a foundation mat besides armorplating. But Keutner, through experiments, proved that foundation mats protect only the upstream of the pier, and serious scour occurs downstream of it. Keutner proposed the use of the pier shape shown in Fig. 24. In

case, a pier of this shape is not available, the following complementary method should be employed:

1. Sharpen the pier nose as much as possible from the foundation to highest water level. ~~The~~ Use ~~of~~ a semi-circular shape above the highest water level.
2. Use steel sheet piling in front of rectangular piers to form a smooth pier nose.
3. Leave sheet piling, used for foundation excavation purposes, after completing the project to prevent deep scour at the nose.

3½p

TABLE OF CONTENT (Part 2)

13

IV THE EFFECT OF PIER ARRANGEMENT ON SCOUR

17 General

According to Dr. Miyamoto, the important factors in considering pier arrangement are as follows:

1. Avoid using a extremely narrow place or a river bend for locating a bridge. The number of piers also should be cut to a minimum.
2. Consideration of the flow direction at flood periods is necessary in constructing a bridge.
3. Piers should be widely spaced such that floods and floating debris can be drained.
4. It is desirable not to construct piers in a narrow river channel.
5. Abutments should not be extended for rivers with banks and consideration should be made in determining the locations of piers for flood treatments
6. Piers built in rivers with a meandering flow pattern or with low water level should be more widely spaced.
7. For parallel dual bridges, it is advantageous to adopt the same pier spacing for both the bridges.

for rivers with banks.

It is difficult to satisfy these factors because of geographic, geologic and economic limitations. Rehbock made model tests for a railway bridge on the River Wilsent, and proposed the use of a pier foundation shown in Fig. 25 (a).

Fig. 25 (b) shows pier foundation actually constructed. They used an octagonal pier foundation on a square caisson, built the pier on it and protected the bed surface with riprap.

The author investigated the effect of pier arrangement on scour. The main experimental terms are listed in Table 13.

18 The Effect of the Angle of Skew Between the Centerline of Flow and the Pier Axis.

A. General

A skewed pier has greater scour and the scour hole is more irregular. However, due to geographic, geologic and economic limitations, skewed bridges are required in some cases. In this case, considering the bridge structure and the characteristics of the river bed and flow, precise considerations should be given in selecting the type of pier to be used. In natural rivers, the direction of flow changes with changing stage, accordingly, it is necessary reasonable to consider diagonal lateral flow to the pier axis in a bridge pier design.

As shown in Table 13 the following models were investigated by the author in his test series G_1 - G_4:

1. Series G_1 - A rectangular pier (30 cm x 15 cm) with two arcs type nose and tail (Type 1 pier) of $2\alpha = 73°44'$ (No. 9) and 123° 52" (No. 5), respectively.
2. Series G_2 - A rectangular pier (30 cm x 15 cm) with semicircular nose and tail (type 2 pier) for comparison with Series G_1
3. Series G_3 - Same pier as in Series G_2, only used critical flow condition with slope = 1/600 and depth = 3.9 cm instead of slope 1/800 and depth 5.2 cm used in Series G_2

4. Series G_4 - Two Circular piers (ϕ = 15 cm) with a spacing of 30 cm (center to center).

The results of series G_1 - G_4 are discussed in B, C, D and E.

Keutner used a pier model having two arc type nose (2α = 101°) and a semicircular tail for his experiments. He placed the model as shown in Fig. 26 and set the run time as 150 minutes. The relationship between the scour widths K_o, K_{fr}, and K_{fl} and the angle of skew is plotted in Fig. 27. The relationship between θ and the scour areas along the two sides of the pier wall, f_r and f_l, and the maximum scour depth, t max, are shown in Fig. 28. The conclusions are:

1. In spite of the fact that there was considerable increase in k_{fr} with an increase in θ, the scour area along the pier wall only slightly increased and the sand piled-up at the tail spreads out over a large area.

   Hence, special consideration for the stability of the right hand side of a pier is not necessary. On the contrary, on the left side of a pier, ~~is increased~~ considerably with an increase in θ though k_{fl} decreased. In general, the maximum scour occurs at the pier nose when θ is small, and As θ approaches 21.5° scour is evident at the tail when θ is 27.0° and the maximum scour shifts to the tail

Thus a pier tends to collapse towards the pier nose when θ is small and, due to the relatively deep scour along the side wall of a pier, when θ is increased, the pier has a tendency to collapse towards a direction parpendicular to the pier axis.

2. If θ is less than 5.5°, the scour pattern is the same as for θ = 0°.

B. Type I Pier: Series G_1

After a careful study of experimental results shown in Figs. 29 to 34 and Tables 14 and 15, the noteworthy conclusions are as follow:

i) A measurable increase in scour k, k' at nose were observed with an increase in θ. Scour depths k_o and k'_o were found to be directly proportional to θ. k_{sr} and k'_{sr} increase very slightly when θ is small but a sudden increase is observed when θ = 10~15°. k_{sl} and k'_{sl} increase rapidly when θ is small and the rate of increment slows down as θ is increased.

The curves k_{fr} and k_{sr}, K_{fl} and k_{sl} have similar relationships with the angle of skew. On the other hand, curve k'_{fl} has quite a different relationship than the others.

ii) Although the scour boundary line $K_o K_{sr}$ K_{sr} on the right hand side of the pier, is parallel to the pier wall S F, the line $K_{sr} K_{fr}$ gradually separates from the pier wall as θ increases. This is due to the effect of eccentricity of flow at the tip of the nose S. On the left hand side of the pier, the scour boundary line K'_o K_o K_{sl} K_{fl} immediately separates from pier wall S F_1. The deviation of the line K_o K_{sl} is very slight when θ is larger than 35°. The line K_{fl} K'_{fl} separates from the pier wall when θ is larger than 40° and the scour fan becomes wider downstream of the pier tail. This widening is due to the eccentricity of flow

of flow and the increase in velocity.

iii) From Figs. 33 and 34, ~~it is important to study the fluctuation of the points K_o and K'_o.~~ The points K_o and K'_o seperate from the center of the pier when θ is less than 25^o and then are constant until θ is 35^o. A further increase in θ again attracts the points near the center of the pier. Points K_{sr} and K_{fr} seperate rapidly from the center line of the flume. However, points K_{sl} and K_{fl} change very slightly due to a change in the angle of skew.

iv) As seen from Fig. 32, there is a great difference in the rate of scour on the right hand and left hand sides of a ~~pier~~ channel. On the right hand side, the scour depth decreases rapidly with an increase in θ and the scour depths t_{fr}, t_{mr} and t_{flr} change signs at $\theta = 18.5^o$, 11.5^o and 9^o respectively. When θ exceeds 20^o the height of pile-up remains almost constant but the scour patterns are different. The line of ~~max~~ maximum pile-up is semicircular around S' when $\theta = 0^o$, and shifts towards Fr' when θ increases (in Fig. 30 and 33, dotted line). The front line reaches point Fr' when $\theta = 20^o$ and passes point M_r when $\theta = 45^o$. On the left side of the ~~pier~~ channel, the scour depths, $t_{s'}$ and t_{fl}, increase with an increase in θ. When θ exceeds 40^o, the scour become more evident. $t_{s'}$ is minimum when θ is about 5^o. Since the scour depth, t_s, at the pier nose S increases rapidly with an increase in θ, it is necessary from the viewpoint of stability to protect the pier nose. When θ is larger than 40^o, t_s increases and t_{fl} decreases. This is because the point of maximum scour shifts from F_t towards S and t_s will become t_{max} when $\theta \fallingdotseq 50^o$.

V) A type I pier with a sharp nose is considered an ideal pier shape when $\theta = 0°$, but scour increases rapidly as θ increases. The scour width on the right side of a pier increases when θ is larger than 10~15°. This condition is not harmful to the stability of a pier.

On the other hand, both the scour depth and the scour width suddenly increase at the nose on the left side of the pier. As a result, scour at the tail becomes evident when θ exceeds 40°. This scour pattern is due to eccentricity of the flow at the sharp nose.

C. Type II Pier: Series G_2

The scour pattern of a Type II pier is different from that of a Type I pier. The results are shown in Figs. 35 to 38 and Tables 16 and 17 (Ref. Fig. 30, 33). The following comparisons of results of Series G_1 and G_2 are note worthy.

i) Scour widths K and K' increase slightly at the nose. But opposite tendencies are observed for curves K_{sr} and K'_{sr} from Fig. 36. Curve K_{sl} is almost similar to K'_{sr} except when θ is small. The fluctuation of K_{fr} is almost similar to that of K'_{sr} when θ is less than 20°. K_{fr} has a slight increase when θ exceeds 20° where as K'_{sr} increases rapidly. Curves for depths K_{fl} and K_{sl} always keep the same relationship with θ, however, curve K_{ji} is quite different from the others.

ii) Scour boundary line $K'_o K_{sr} K_{fr}$ has a similar shape close to the pier wall at the nose but gradually parts from the wall downstream of pier. Near the point K_{sr} the boundary line tends to come close to the wall but the boundary line downstream from K_{fr}

seperates rapidly from the wall when θ is larger than 30°. This is because eccentricity of flow at the semicircular nose has been less effective flows along the pier wall. The evident seperation of the boundary line from the wall, when θ is larger than 30°, is due to the sudden expansion of the flow width at F_r.

On the left hand side of the channel pier, the scour boundary line $K_o' K_{sl} K_{fl}$ at the nose has approximately the same shape as S F_r but gradually seperates from the wall at the downstream end of the pier. When θ exceeds 20 ~ 25° the line K_{sl} K_{fl} parts from the wall and the scour width at the tail increases. The region of scour spreads out over a large area when θ exceeds 30°. This is due to the effect of eccentricity of flow at the pier nose , (in the pier nose tested, the effect of eccentricity is not affected very much by a change in the angle of skew) and the increase in velocity.

iii) Using the center of the pier and the center line of the flume as a base (Fig. 33), the results of the tests are replotted in Fig. 38. The point K_o separates from the center when θ is small and approaches the center when θ is approximately 15°. K_o' has no change when θ is small and rapidly approaches the center as θ increases. The points K_{sr} and K_{fr} on the right side of the channel pier seperate from the center line very quickly but the rate of seperation is far less than that for a Type I pier. On the contrary, points K_{sl} and K_{fl} on the left side of the channel pier approach the center line when θ is less than 20 ~ 25° and then seperate as θ gets bigger. The following comparison of the scour pattern for a Type I and Type II pier can be made. Points K_{fl}' and K_{fl} except, when θ is less than 10°, have similar fluctuations

with respect to θ and the scour boundary is parallel to the pier wall on the left side for both type of piers.

iv) Comparing Figs. 32 and 37 it is seen that the two type of piers have different trends for the rate of scour. A decrease in the scour depths t_{fr}, $t_{f'r}$ and t_{mr} on the right hand side of the channel pier are observed. The fan representing the maximum deposit is semicircular around s' when $\theta = 0°$, but shifts toward $F'r$ when $\theta = 35 \sim 40°$.

The scour depths on the left side, particularly t'_s and $t_{f'\ell}$ increase with θ, although, t'_s and $t_{f'\ell}$ show only a relatively mild increase when θ reaches 30°. This is due to a reduction in the fluctuation effect of flow eccentricity, by rounding-off the tail shape. The value of $t_{f'\ell}$ is maximum when θ is 45° but t'_s becomes maximum when θ is about 5°.

The scour at the tip of the pier nose, t_s, increases with an increase in θ. When θ reaches 30°, t_s tends to decrease. This is due to the shifting of the maximum scour, t_{max}, from the tip towards $F\ell$. This pattern is very evident when θ is larger than 30°. t_{max} occurs at the point on the pier nose which is directly facing the flow and the value of t_{max} is nearly constant when θ exceeds 20°.

v) A Type II pier is desirable when θ is large, because the skew angle has relatively little effect on the scour depth around this type of pier. The scour hole on the right side increases in width when θ is larger than 30°, but this is not harmful to pier stability as the scour depth is reduced.

On the left side of the channel pier a mild increase in the scour depth and the scour width are observed at the nose. At the pier

tail, the scour depth increases, and the scour width decrease increases little rapidly when θ approaches 30°. It is worthwhile noting that the maximum scour shifts to the tail when θ is about 45°. The discussion just completed are the conspicuous differences between a Type II and a Type I pier. These differences are, due to the rounding of the nose and tail of the pier so that there is no evident change in the eccentricity of flow by increasing the skew angle.

D. Type II Pier: Series G_3

Series G_3 was run under different criticla flow conditions but with the same pier model as series G_2. The test results are shown in Figs. 39 to 41 and Tables 18, and 19. The following comparison can be made with series G_2.

i) The scour patterns for series G_2 and G_3 are very similar and the fluctuation of the scour with respect to θ is alike for the two series. This show that the condition of flow does not affect the scour pattern. Thus, it is suggested that the qualitative results from these tests can be applied in the field.

ii) The values of scour depths and scour widths for series G_3 were less than those observed for series G_2. From the results, it is considered that the scour depth and scour width decrease with a decrease in the depth of flow. This conclusion varify the findings of Series A_1 and B[(10)c].

The rate at which the scour decreases with respect to the depth of flow becomes evident as the skew angle gets larger. If $\underline{K}$ and $\underline{t}$ are the differences of scour depth and scour width between the two series G_2 and G_3, it is seen tha, $\underline{K}$ and $\underline{t}$ increase grad-

ually for θ = 0 - 30°, but after θ exceeds 30°, no difference between the two series is recognized. This is due to eccentricity of flow and other complex hydraulic phenomenon. The detail is discussed in the next report.

E. Two Circular Piers: Series G_4

The scour pattern, except at the front part of the pier, of series G_4 is quite different from those of series G_2 and G_3.

Tables 20 and 21 are a tabulation of the data for scour depth and width for Series G_4. The symbols are shown in the definition sketch, Fig. 43. When two circular piers with a large skew angle are used, each pier directly faces the flow and thus acts as an individual pier.

In order to study the relationship more closely, the author assumed each pier as an individual pier and determined the scour width and the scour depth at each corresponding point which are shown as K^o and t^o in Fig. 43 with dashed lines. The scour width in table 20 and the scour depth in table 21 are tabulated in Table 22 and plotted in Figs. 49 and 50.

The following are the noteworth conclusions from Figs. 43 to 50.

i) The scour depths k_o and k'_o increase with an increase in skew angle, θ (Fig. 44). When θ is larger than 20-29° the rate of increase of k_o decreases and k'_o decreases in magnitude. The scour depth k_{sr} on the right side of the channel decreases with θ, whereas, k'_{sr} increases rapidly, especially when θ is larger than 25°. On the other hand, $k'_{s\ell}$, the scour depth on the left side has a direct relationship with θ and $k'_{s\ell}$ is almost independent of θ.

Although, k_{fr} for the front pier has an increasing straight line curve with respect to θ, K_{fl} shows only a slight increase. $k_{f'l}$ for the rear pier decreases rapidly when θ is small but shows an increase at $\theta = 25^{\circ}$ and then has approximately the same tendency as $k_{f\ell}$. $k_{1\ell}$ decreases for $\theta = 0\text{-}25^{\circ}$, then increases with θ. The increase in the value of $k_{1\ell}$ is evident when θ reaches 35°. In general, the sand scoured from the upstream side of the front pier will pile-up on the bed between the two piers, however, the sand will be washed downstream because of the scouring around the rear pier. In Fig. 48, M represents a marginal point which is directly affected by scour around the front pier and M' represents a point which is affected by tractive effect of flow due to the rear pier. If $\overline{Ma} = a_m$ $\overline{1M'} = K_{m'}$, The variations of points M and M' with respect to the skew angle are plotted in Fig. 44. Point M seperates from point 2 as θ increases and is at the mid point of 1 and 2 when θ is about 15°. This point moves back towards point 2 until θ exceeds 30°, then the point seperates from 2 again.

Point M' does not move when θ is $15 \sim 30^{\circ}$ but begins to move towards point 1 when θ exceeds 30°.

ii) It was reported in the previous report that the scour pattern for two circular piers, ($\ell_1/b = 1 \sim 2$), parallel to flow, is the same as that for the wall Type pier. From the above statement, it is suggested that two circular piers with a small skew angle may be considered as a wall type pier. Based on this assumption, comparisons on the scour patterns of series G_4 and G_2 and G_3 can be made as follows:

The fluctuations, in series G_4, of widths k_o, k'_{sr}, k_{sr}, $k_{s\ell}$, k'_{sr} and $k'_{s\ell}$ with respect to θ, are similar with those for the Type II pier when θ is less than 5-10°. A further increase in θ does not have any particular effect on the scour width on the right side of the channel, however, a measurable charge is observed on the left side of the channel. Although k_{fr} and $k_{f\ell}$ for the front pier shows a different variation with θ from that the type II pier, the variation of k_{fr} is not evident. $k_{f\ell}$ on the left side, shows considerable difference when θ exceeds about 25°. This pattern is closely related with vertical eddies which exist between the two piers.

When θ is small no change in the eddies is observed, but as θ increases the eddies move towards the right of line 1-2. The movement of eddies, as θ increases, reduces their effect on the rear pier. At θ = 25°, this reduced effect is evident and each pier acts as an individual pier.

iii) If it is assumed that the two piers act as individual piers, the variation of scour width k'^{o}_{o} is as follows:

At the front pier, inspite of a slight increase in k^o_o, k^o_{sr} and $k^o_{s\ell}$ have a tendency to decrease ($k^o_{s\ell} < k^o_{s\ell}$), and the scour width k^o_{fr} and $k^o_{f\ell}$ show a slight decrease ($k^o_{fr} < k^o_{f\ell}$). This is because the front pier acts as an individual one and also as with increase in θ and the rear pier has little effect on the scour width. $k^o_{1\ell}$ and $k^o_{f\ell}$ also increase suddenly when $\theta \geq$ 25°, and 30° respectively. This is because the rear pier acts as an individual pier and the result of the effect of scour at the front pier.

iv) Fig. 49 is a plot of the variations of the scour width using pier centers and flume center line as a base. Comparing with series G_2 and G_3 for the wall type pier, it is found that similar relationships as written in ii) exist.

v) Fig. 45 is a plot of the scour depth t. The following are the essential conclusions derived from Fig. 45: The scour depths at the front and the sides (t_s, t_{fr} and $t_{f\ell}$) of front pier are the same as in series G_2 and G_3 for the wall type pier. When θ is small the scour depths at the sides, $t_{f'r}$ and $t_{f'\ell}$ of the rear pier are no different from the wall type pier. Hence two circular piers, as a whole, can be considered as a wall type pier when θ is small.

t_{ℓ} and t'_m remain constant when θ = 15~35°. This is due to a balance of the tractive effect and the piling effect of the flow. When θ reaches 35° the tractive effect become more pronounced, thus t_{ℓ} and $t_{m'}$ increase.

The reason t_2 and $t_{f'\ell}$ keep constant when $\theta \fallingdotseq 20°$ is the same that for t_{ℓ} and $t_{m'}$ remaining constant. A further increase in θ causes an increase in $t_{f'\ell}$ and it approaches $t_{f\ell}$. On the contrary $t_{f'r}$ decreases when θ reaches 20° due to the scouring effect, and then $t_{f'\ell}$ decreases again at θ = 35° due to the piling effect caused by the eddies behind the rear pier.

The scour depth $t_{s'}$ at the rear pier has the same variation as the tail of a wall type pier. It approaches the value of t_{ℓ}, when θ is extremely large. However, the more the rear pier acts as an independent pier, the greater will be the scour depth around it and the more harmful the pier will be to its own stability.

vi) Assuming the two piers as individual piers, the scour depth t^o is as shown in Fig. 47. The pattern of increase of t_s^o, t_{fr}^o, $t_{f\ell}^o$ and t_ℓ^o with respect to θ is corresponding to that of the wall type pier with a shorter pier length. This means that the front pier shows up the characteristics of an individual pier. Because of the effect of the rear pier on the left side of the front one, the scour depth $t_{f\ell}^o$ is greater than t_{fr}^o. The increase of t_2^o, $t_{f'\ell}^o$ and $t_{s'}^o$ when θ is larger than 5^o, shows that the rear pier acts as individual one. The piling up of sand behind the front pier is the reason for the slight change in the values of t_s^o and $t_{f'\ell}^o$, when $\theta = 20 \sim 35^o$. However, as θ exceeds 35^o the rear pier acts as an individual pier more and more and t_s^o and $t_{f'\ell}^o$ increase gradually and approach the values of t_s^o and $t_{f\ell}^o$ respectively. ~~Finally,~~ And also the values of t_s^o ~~and $t_{f'\ell}$~~ coincides with ~~those of $t_{s'}^o$ and t_ℓ^o~~ that. ~~t_{fr}^o has the same tendency as $t_{f'r}$ in v), when θ is less than 35^o, but as there is piling effect due to eddies at the rear pier the value of t_{fr}^o.~~

vii) When θ is less than 5^o it has no effect on the scour. The scour almost remains constant when θ is 15^o - 35^o but the scour depths behind the front pier and the upstream part of rear pier increase with θ.

However, the rear pier acts as an individual pier when θ is larger than 35^o which is harmful to its own stability. The disadvantage of using two circular piers is the effect of θ on the scour between the two piers.

F Conclusion

Since series G_1, G_2, G_3, and G_4 were performed based on previous experimental results (9), the change in scour pattern among the different series can be attributed only to the skew angle of the piers. This statement was verified in series G_2 and G_3 under different flow conditions. Hence the results of the experiments are found to be qualitatively reliable. The skew angle does not affect bed scour only when θ is slight, but the scour, both at the nose and at the tail, increase with θ. This rate of increase is largely governed by the pier shape. For example, the rate of increase of scour for the wall type pier with a circular nose and tail is less than that for a pier with a sharp nose, when θ increases. In the case of two circular piers, there is no effect on the upstream side of the front pier, but the scour of the bed between the two piers increases with θ. Keutner's experimental results Figs. 26 ~ 28 show that when θ is less than 5.5° the scour pattern is the same as that for a pier with no skew angle to flow. This coincides with the authors findings, though However, it is difficult to compare Keutner's and the author's experiments for different shapes of piers. A measureable difference has been observed in the variation of t_{max} and on whether $k_{fr} > k_{f\ell}$. This difference may be because Keutner neglected to consider bed materials, and thus the differences in scour pattern among Keutner's experiments may not be only due to the effect of skew angle.

19 The Effect of Opening Ratio

A. General

When the opening ratio b/D, the opening D and width of pier b, is small, each pier acts as an individual pier and when the b/D ratio is too large, it is not applicable to field. For these reasons, the author used D/b = 60.67~6.07 for series Hn. Five model scales were used (n = 1, 2, 3, 4 and 5). H_1 is ~~the results~~ for a standard model (ℓ_1 = 30.0^{cm} and b = 15.0^{cm}). Hn is the ~~results~~ tests for a model of $\ell_1 = \frac{30}{n}$cm, b = $\frac{15}{n}$cm. 3 x H_3 represents three piers of ℓ_1 = 10^{cm} b = 5^{cm}. Hn_I and H_{nII} represent the series for a type I ~~pier~~ and a type II pier respectively. All the experiments were performed under critical condition (a) with a test time of 20 minutes.

The following are results of the experiments.

B Type I Pier: Series H_{nI}

Tables 23~27 are the tabulation of the data observed during the tests. The type of pier are as shown in Fig 51 and the symbols are those shown in Fig 11 of the previous report. The solid line in Fig. 54 represents the scour width for the pier ① which is nearest to center line (assumed as a typical one). If pier ① is not on center line, the scour width is less than that at the center line. This is due to the velocity distribution of the flow. These facts can be seen from Figs 23-27. Figs. 55 and 56 are the scour widths, k_s and k_f and Figs. 57 and 58 are the scour depths, t_s and t_f, for pier ① .

The noteworthy conclusions from these figures are as follows:

i) Scour widths k_o, k_s and k_f and scour depths t_s and t_f slightly increase with a decrease in the ratio D/b. This increase in scour was observed for the large models H_{1I} and H_{2I} only when D/b was less than 10. Hence, it is recognized that the effect of pier spacing is negligible when D/b is larger than 10.

The backwater caused by a pier is considered as having a serious effect on scour at the nose, but the scour is also governed by the eccentricity of flow at the pier nose and if D/b is not extremely small this eccentricity of flow has no evident change. This is considered as the main reason for k_o, k_s and t_s changing slightly. The velocity of the flow between the piers will increase with a decrease in D/b, but no additional scour on the bed between the piers was observed in the experiments as seen from Fig 53. This is because critical condition of flow were used and only a little additional scour is expected under higher velocities than that for critical flow conditions. The scour at the transition point increases with an increase in velocity due to flow along the pier wall. The flow is pushed back near the point F, thus creating vertical eddies which the piling of sand. This phenomenon is more rapid when D/b is small, and t_f and k_f have a tendency to decrease with a decrease in D/b is considered a balancing phenomenon, between the eccentric

flow and the pushing back effect of the flow. The scour pattern at point F' is explained in like manner. It is reasonable to consider the fixed value of t_s, as the result of a slight fluctuation in the eddy. Nevertheless, it is necessary to pay attention to the fact that the increase in the scour due to a decrease in D/b is slight. If the ratio D/b is extremely small, the eccentricity of flow and the velocity of flow will increase rapidly, such that a slight increase in scour can not be avoided.

ii) If two piers are inserted in flume, the scour for the pier which is near to center line is more pronounced than that for the other. This is because of the velocity distribution in the flume. These facts can be seen from Tables 23~27.

iii) In general, for turbulent flow, the direction and intensity of velocity at a point is not constant. Thus, the velocity at a point is the mean velocity over a time period. The flow is not always divided regularly on both sides of a bridge pier. The fluctuation of the intensity of flow can be observed from the movement of the sand particles at the tip of the pier nose. Since this phenomenon is interrupted by flume wall, the scour on the bed near the wall downstream of the pier is decreased.

C Type II pier: Series H_{nII}

The results of this series is shown in Fig. 59 and Tables 28~32. For comparing the scour widths k_o, k_s and k_f and scour depths t_s and t_f, with respect to D/b, for the Type I and II pier, the data is plotted in Figs. 54~58 as a dashed line.

The following facts are observed:

i) The tendency for the scour to increase in magnitude with a decrease in the ratio D/b is slightly larger for a type II pier than that for a Type I pier. The scour for this type of pier is greater from the beginning, hence, the rate of increase is approximately similar to the others. Regardless of the nose shape, the ratio D/b has no effect on the scour at the tip of the nose. This fact is the same as for the scour depths t_f' and t_s' at the pier tail. Moreover, the conclusions stated in ii) ~~and iii)~~ of (B) are also recognized in this series.

ii) As is evident from Figs.54~58, both the scour depths and the scour widths are less for a type I pier than that for a type II pier. The difference in the scour pattern between the two types of piers, is evident for the scour width k_o and k_s and the scour depth t_s, which are mainly governed by the eccentricity of the flow at the tip of the nose. Only a slight difference is observed for k_f, t_f, t_f' and t_s', between the two types of piers tested.

D Conclusion

Since series H_{nI} and H_{nII} were performed under the same critical conditions (α) with a test period of 20 minutes, the different pattern for scour for the two series may be considered as due only to a change in the ratio D/b. The ratio D/b affects the scour at the nose and tail, for any shape of pier, only when D/b is less than 10~15. The effect of D/b on scour, it was found, had been overestimated in the past ~~previous experiments.~~ Thus, it is reasonable to determine suitable spacing for piers by considering

the geography of the site, and the geologic and structural aspects of the problem.

Backwater should be considered in the pier construction but it does not seem important from the point of scour. The relationship between velocity distribution and the scour, and the scour pattern of the pier which is near the bank were also studied. It was found that a Type I pier (sharpen nose) was more advantageous than a type II pier.

20 The Effect of a New Bridge Constructed Near an Existing Bridge

A General

With advancement in the field of transportation, a parallel arrangement of bridges can not be avoided in some locations.

Timonoff made experiments on dual bridges at the Leningrad experimental station. He made the ~~following~~ suggestions described in (13) for guidance in the design of parallel dual bridges.

a. Since the stability of a pier is mainly governed by scour at the pier nose, it is desirable to locate a new bridge down stream of the existing one, if the foundation of the existing bridge is deep; and to construct it upstream of the existing bridge if the foundation is shallow.

b. The new bridge should be located upstream of the existing structure if the spacing of the piers is larger than that of the existing bridge and to construct it down stream if the spacing is smaller.

In the following, the discussion of results of Series F and G_4 is made comparing with Timonoff's suggestions.

B Discussion of Results of Series F and G_4:

Series F and G_4 are for two parallel circular piers. It is possible to suggest the scour pattern for two wall type piers, which are built parallel to flow from the results of the parallel circular piers. The following is the author's opinion based on the result of these series:

1) As stated before, the disadvantage of the two circular piers is the considerable scour that occurs between the two piers. But when $l_1/b \approx 2/3$ scour and the piling-up of the bed material are in equilibrium and the bed surface is kept almost at the original state.

However, the scour ~~on both sides~~ at the tip of the rear pier will affect ~~increase~~ that behind the front pier if l_1/b is ~~less than 2; thus, affecting the stability of the rear pier.~~ too small.

The piling-up of sand is more evident for the wall type pier than for the circular pier. Accordingly, 1 – 2 times the pier width is proposed as the distance between two wall type piers.

ii) It is seen from series H_n, that a change in the ratio D/b has slight effect on scour when D/b is larger than 10~15. Suggestion 2/) given by Timonoff seems to overestimate the effect of pier spacing. Hence, it is enough only to consider the geography and the geology before constructing a new bridge, except when D/b has an extremely small value.

iii) From the experiments on the effect of skew angle on scour around two circular piers, it was seen that θ had no

effect on the scour when it was less than 5°.

Accordingly, when a parallel arrangement for a new pier and an existing pier is difficult in the field, it is not harmful to scour to arrange the piers such that the line connecting the centers of the two piers makes an angle less than 5° with the flow. Also, the longer the pier, the mofe effect it will have on the bed. In case, $\theta > 5^{\circ}$ can not be avoided, it is desirable to have a long distance between the two piers, (at least 4 times the pier width) so that each pier may act as an individual pier.

21 Conclusions

From the viewpoint of pier arrangement, measures for reducing the scour on the bed are as follows:

i) Scour will increase with an increase in the skew angle. Accordingly, the pier axis should be parallel to the maximum flood flow and the skew angle at any other discharge should be less than $5 \sim 10^{\circ}$.

ii) The effect of pier shape on scour increases with θ. When $\theta = 0$, the sharper the nose the less the scour; on the contrary, the sharper the nose the more the scour as θ increases. Accordingly, for a river in which the flow direction is changeable, it is advisable to construct a pier with a semi-circular nose. Moreover, it is also recommended that two circular piers, with a skew angle and a large spacing not be used.

iii) For any nose shape for the wall type pier, the ratio D/b has a slight effect on the scour around the pier, when D/b is less than $10 \sim 15$. Hence, it is reasonable to determine the

bridge span based on geographic, geologic, and economic conditions rather than on scour.

iv) More scour occurs around a pier at the center of the river than around one near the bank. This means that there is a close relationship between the flow velocity and the scour.

v) For the construction of a new bridge near an existing bridge, the following factors are suggested as a guide for design:

a) The pier axes should coincide

b) Examine the foundation of the existing pier, to determine the location of the new pier (upstream or downstream)

c) The distance between the two piers should be about twice the pier width.

d) When it is difficult for the pier axes to coincide, it is desirable that the angle between the line connecting the center of the piers and the flow be less than 5^{o}. If this is still impossible, it is suggested that the two bridges be located as far apart as possible.

TABLE OF CONTENT (Part 3)

5. The application of experimental results to actual field problems.

(22) The effect of model scale

A. General

No definite conclusions regarding a law of similarity for a fixed river bed is yet available. Hence it is difficult to establish a reliable law of similarity for local scour around bridge piers. Thus it is impossible to arrive at quantitative conclusions from the experiments. By referring to series K_1, K_2 and K_3, the reliability of the experiments performed can be shown. Herein is a discussion on the effect of model scale.

B. A study on the results of series H_{nI} and H_{nII}.

Since series H_{nI} and H_{nII} were run for the same time period (20 minutes) and by using the same material, the difference in scour pattern between them could be attributed only to the model scale for equal values of D/b. The scour data for D/b = 12.19 from Talbes 23-32 is rewritten in tables 33 and 34. The scour depth and width are plotted against model scale 1/n in Figs. 60-61. The solid line represents a type I pier and the dotted line stands for a type II pier. The following are the noteworthy conclusions derived from the above plot:

i) Scour width k_o, k_s and k_f will decrease with a decrease in model scale. Judging from the fact that the scour phenomena varies with pier shape and the point at which the measurement was taken, the scour around a pier results from complex mechanics, and thus it is difficult to establish a perfect law of similarity for pier scour. But it is desirable for obtaining reliable quantitative data to make a model as large as possible.

If the horizontal scale is 1/20 and the vertical scale is 1/40 for a model of l_1 = 30 cm and b = 15 cm, the corresponding prototype size is 6 m x 3 m with a full length of 13 m for a type I pier and 9 m for a type II pier. The pier spacing is 1.82 x 20 = 36.4 m, and the depth of flow is 0.052 x 40 = 2.08 m. Applying Eq.12 of the first report, e = $40^2/20$ = 80 . Thus the mean diameter of the sand particles is 0.0708 x 80 = 5.664 cm. Using Fig. 60, it is possible to suggest data for practical use, but since there is no perfect law of similarity for the scour width, it is difficult to obtain precise values of scour width. As shown in Fig. 60, the scour for a type I pier is less than that for a type II pier and this fact becomes more evident as the model scale approaches 1 . The scour width, k_f , for a type I pier, decreases slightly with a decrease in 1/n . This is due to the effect of scour at the pier nose extending downstream of of the pier when the model is small and thus lessening the effect of sand pile-up behind the pier. A similar pattern was observed for the widths k_f and k_s when a type II pier was tested. From these observations it is seen that the scour mechanism changes when the model is small. Hence, for a model having a model scale less than 0.50, qualitative conclusion may be unobtainable.

ii) From Fig. 61 it is evident that scour depth is equal to zero when 1/n is zero. However, the figure also shows different scour phenomena for different values of 1/n and different pier shapes. It is difficult to establish a perfect law of similarity. Judging from the fact that a type I pier is superior when 1/n $\doteqdot$ 1 , it is suggested that a type I

pier be used in the field. As shown in Fig. 61, the scour depths t_f and t_s at the pier tail decrease with an increase in $1/n$, yet it is still difficult to predict the scour phenomena for an actual pier in the field. It is also recognized that the data for the scour phenomena, when $1/n$ is small, are unreliable due to scouring effect at the pier nose.

C. Conclusion

The following conclusions can be made from series H_{n_I} and $H_{n_{II}}$:

i. The scour depth and width become zero when $1/n$ is zero.

ii. A perfect law of similarity for these experiments is difficult to establish.

iii. It is necessary to use models as large as possible for obtaining qualitatively reliable data.

iv. It is difficult to obtain reliable data from models, having extremely small model scales.

(23) The effect of bed material

A. General

In order to obtain qualitatively reliable conclusions, it is necessary to compare the experimental results for different materials.

B. Sand from River Kizu

The sand from R. Yasu, used in previous experiments, was compared with sand from R. Kizu for studying the effect of bed material. The sieve analysis of these sands is shown in table 35 and Fig. 62. Table 36 shows the results of the preliminary experiments for the determination of

critical tractive force. Inspite of the fact that the mean diameter of the Kizu river sand is 0.921 mm and that of the Yasu river sand is 0.708 mm, critical conditions for the Kizu river sand were reached at comparably shallow water depths. This is due to the small proportion of fine materials, as seen from Fig. 62. These results show that the consistency layer density of sand has a close relationship with critical tractive force. Ripples were not so evident for the Kizu river sand after critical conditions were established. This is also considered as resulting from the smaller proportion of fine material. As for Yasu river sand, the Kizu river sand also shows a fixed value of critical tractive force for all slopes. From this statement, the basic concept of the tractive force theory is also proved.

The following is a comparison of the experimental data (Table 36) with the values computed by applying Kramer and Indris' experimental formulas (Table 35).

Although the computed value (Kramer's formula (10)) 64.15 g/m^2 and the experimental value 65.11 g/m^2 are close for the Yasu river sand, these show a 18.7% deviation (63.16 g/m^2 and 53.22 g/m^2) for the Kizu river sand. A similar relationship is observed by comparison with values computed using Indris' formula (11). These are due to errors in the determination of the coefficient. Kramer also recognized 15% error in his formula.

Since the specific gravity of the Yasu river sand and the Kisu river sand are the same, F_o computed from Eq (10) must be proportional to dm/M .

According to the formula, $F_o = k(w - w_c)\lambda_{dm}$, propsed by Aki and Sato, F_o is proportional to λ_{dm}. λ is the weighted ratio of the particles having diameter smaller than the mean diameter to the particles having diameter larger than mean diameter.

Although it is difficult to obtain a definite conclusion from experiments for only two kinds of bed material, it can be observed from table 37 that the ratio of F_o is different from the ratio S_{dm}/M and λ_{dm}.

From the fact, it is known that Kramer's formula and Aki and Sato's formula are not appricable and further study on density is needed. There is no proper experimental formula for expressing the relationship between critical tractive force and the bed material. However, from table 36 it is recognized that the basic concept of the tractive force theory is reliable.

Based on the above statement, $F_o = 53.22\ g/m^2$ is used for the Kizu river sand and critical conditions are as in Table 38. On computing the velocity coefficient C and the coefficient of roughness $\frac{n}{N}$, the hydraulic radius R is assumed equal to the depth of water H.

In order to avoid the formation of ripples, Kray proposed $d/8H < 1$ for Eq (13) in Chapter (7). But it is difficult to determine d for this bed material due to the high proportion of fine particles. However, ripples were not formed within the 20 minutes test time. Thus it is reasonable to consider that the critical conditions for these experiments satisfy the condition $d/8H < 1$.

From Table 38, it is evident that the critical condition also satisfies $I < g/c^2$ and $V < \sqrt{gH}$ which are the limit of rapid flow.

C. Experiments on Kizu river sand

Results of experiments on Kizu river sand are listed in Table 39.

D. Series K_1, K_2 and K_3

The scour phenomena is similar to that for series H_{n_I} and $H_{n_{II}}$. The results are shown in Tables 40~44 and Figs. 63~67. The noteworthy conclusions are as follows:

i) The fluctuation of the scour phenomena shows different trends for each point of measurement when $1/n$ changes. Accordingly, it is difficult to establish a perfect law of similarity and experimental results give only qualitative conclusions. When $1/n$ is extremely small, the reliability of the qulitative conclusions decrease considerably due to the change in the scour mechanics at the downstream end of pier.

ii) For a type I pier, in general, K_s and K_f are larger than K_o and $K_s < K_f$. These values increase with an increase in $1/n$, and the magnitude is in descending order as K_o, K_f and K_s.

When $1/n \approx 0.5$, the tendency of increases for K_f slows down and when $1/n$ approahces the prototype it is suggested that K_s will be larger than K_f. For a type II pier $k_o < k_f < k_s$ and the tendency to increase is in the order k_s, k_f and k_o when $1/n$ is small. After $1/n$ reaches 0.5 the tendency for k_f to increase slows down and k_f approahhes k_o. This is due to, as stated before, the piling effect caused by vertical eddies at the downstream end of the pier.

The scour depth t_s is less than t_f for a type I pier but t_s is larger than t_f for a type II pier, although the increase in t_f, with an increase in $1/n$, is less than that of t_s. Hence, it is expected that t_f approaches t_s when $1/n$ gets larger. Therefore it is concluded that a type I pier is more advantageous than a type II pier from the point of scour.

The scour depths t'_s and t'_f decrease with an increase in $1/n$ and any further increase in $1/n$ causes a pile-up of sand at the pier tail. Scour depth t'_s and t'_f for a type I pier are less than that for a type II pier. This shows that the pile-up of sand at the tail becomes evident as the pier tail is sharpened.

iii) Observing the changes of scour phenomena for different critical conditions it is seen that the larger the depth of flow, the larger the scour depth and scour width. However, the rates of change of scour due to pier shape and model scale are similar to one-another.

E. Comparison of series K and H

Series K is run for models of different scale and the results are plotted in Figs. 63-67. By comparing Figs. 63-67 and Figs. 60-61, the following conclusions are derived:

i. The changes of scour phenomena caused by pier shape and model scale are almost similar and the statements made in i) and ii) of the previous chapter also hold good for series H for Yasu River sand. In the light of the above statements, it is considered that the same conclusion can be obtained from experiments using different sizes of bed materials.

ii. The critical tractive force for the Kizu River sand is 53.52 g/m^2 and that for the Yasu River sand is 65.11 g/m^2. If the law of similarity, which was studied in Chapter 7 of the first report, can be applied to the scour around piers, then it is seen that the scour for the Yasu River sand is less than that for the Kizu River sand. However, precise measurements of scour at different points show that there is no fixed relationship for scour between the two series when 1/n is less than 0.33; that is, the differences fluctuations of scour widths k_s and k_f for a type I pier becomes evident, whereas the differences fluctuations of scour depths t_s and t_f for a type II pier and t_s for a type I pier becomes less. Thus series k_3 has larger values than series H. The scour depth t_s' for series k_3 begins to decrease when 1/n is less than 0.25, and that for series H begins to decrease when 1/n is less than 0.20. It is observed that there is a greater difference between the prototype and model when a small 1/n is used for the tests, thus making it more difficult to arrive at qualitative conclusions. This is caused by a change in the scour mechanics and also by a change in the angle of repose of the sand.

F. Conclusions

Since different sand sizes have no effect on the scour for a particular model scale, and also the changes in scour phenomena due to pier shape are unaffected by critical conditions, it is proved that the author's experiment reported previously have qualitatively reliable results.

(24) The effect of critical conditions

A. General

For the purpose of investigating the effect of nose shape on scour, series A_1 and B were run using Yasu River sand under critical conditions (a) and (b). Series G_2 and G_3 were for investigating the effect of skew angle using the Yasu River sand.

For Kizu River sand, series K_1, K_2 and K_3 were run for investigating the effect of pier shape and model scale on scour, under critical conditions of (q), (r) and (s). The comparison between the series are reported in (B), (C) and (D). Since the depth of flow are 5.2 cm, 3.9 cm, 8.0 cm, 5.3 cm and 4.3 cm for the critical conditions (a), (b), (q), (r) and (s) respectively, it may be said that an investigation on the effect of critical condition for a sand is the same as investigating the effect of vertical scale.

By combining these results with those in Sec. (22), it seems possible to discuss to a certain extent the horizontal and vertical scale effects of model scale. However, from the point of the law of similarity, it is difficult to make a definite conclusion. This statement can be easily understood from Table 38. Despite the increase in slope with an increase in depth (vertical scale), the slope was less for critical conditions with large flow depths. In general, this means that a change in vertical scale not only means a change in vertical scale but also a change in slppe. Thus it is difficult to discuss obtain the effect of vertical scale on scour.

Based on the concept that the bed resistance is proportional to tractive force, the slope in the natural river is recognized to have a close relationship with tractive force. The author insists that the critical flow conditions

for a river slope has a relationship with maximum flood. From this point, it is reasonable to consider the experimental results for tests performed under critical conditions correspond to flood flow conditions.

B. Comparison of series A_1 and B

i. As shown in Figs. 12, 13 and 17 of the first report, the effect of various pier nose shapes on scour for a particular bed material under different critical conditions of flow resemble one another. This fact proves the reliability of the qualitative conclusions derived from these experiments and, by combining with the concept stated in (A) it is suggested that the results of these experiments may be applied in the field with confidence.

ii. Assuming that the law of similarity for the tractive force theory can be applied to local scour around piers it is seen that the scour phenomena for the different critical conditions of flow is quite similar for a particular bed material, regardless of the depth of flow. However, the scour for series B is less than the scour for series A_1, by about 90%. Hence it is evident the law of similarity for the tractive force theory cannot be applied to the scour problem. Nevertheless, it is observed from series A_1 and B that the scour is less for the critical condition with the shallower depth. This is also true for series G_2 and G_3 and series K_1 (k_1), K_2 (k_2) and K_3 (k_3) for Kizu River sand.

For series B and A_1, the depth ratio is 3.9/5.2 = 0.75 and the scour ratio is about a cube root of the depth ratio ($\sqrt[3]{0.75} = 0.909$) and it seems to show some particular relationship, yet the scour ratios are different for the various point where measurements are taken.

The facts stated above show that a law of similarity for the scour problem is difficult to establish. This is due to the change in the scour mechanics with different nose shapes; also the effect of the angle of repose of the sand layer becomes evident by sharpening the pier nose.

C. Comparison of series G_2 and G_3

i. As shown in Figs. 36-38 and 39-41, the effect of skew angle on scour for a particular bed material, regardless of critical conditions, are similar.

ii. Less scour, both in depth and width, is observed for critical conditions with shallow flow depths.

D. Comparison of series k_1, k_2 and k_3

i. As shown in Figs. 63-67, the effects of pier shape and scale on scour for Kizu River sand under different critical conditions are similar. The same phenomena can also be observed from Figs. 60 and 61 for Yasu River sand under critical conditions.

(a) Judging from the above statement, the conclusions for Yasu River sand stated in the last two chapters are applicable for different bed materials.

ii. The relationship between scour and the depth of flow is the same as (B) and (C). The flow depth ratio for series k_3 and k_2 is 4.3/5.3 = 0.8. Scour ratios are 0.867 for a type I pier and 0.945 for a type II pier (average values were taken from the data of runs having model scales of 1.00 and 0.50).

E. Conclusions

The effects of pier shape, scale and skew angle on scour for different bed materials under different critical conditions are fairly similar. This fact proves qualitatively the reliability of the experimental results reported in the last two chapters.

The scour will decrease with a decrease in the flow depth. However, the rate of decrease is related to the characteristics of the bed material, pier shape, scale of model and the point of measurement. Hence it is difficult to establish a perfect law of similarity and to obtain quantitatively a conclusion for the scour problem.

(25) Conclusions

Since the experiments were run for a period of 20 minutes and considering the difficulties in obtaining a perfect law of similarity, it is necessary to give special attention for field applications. In order to obtain reliable qualitative conclusions, the author discusses the effects of model scale, bed material and critical conditions on scour and gives the following opinions:

i) Regardless of bed material, the scour will be zero when the ratio $1/n$ approaches zero. From this point, the scour is considered as resulting only from the existance of piers.

ii) Although a large model scale gives more reliable conclusions, nevertheless, the scour phenomena in the field can be qualitatively suggested using the author's experiments as a guide. The prediction is more accurate when

the scour is mainly controlled by the eccentricity of flow and is less accurate when scour is affected by the piling-up of sand caused by vertical eddy. If the model scale is extremely small, even qualitative conclusions cannot be expected due to the change in the scour mechanics, and the angle of repose of the sand layer.

iii) The effect of pier shape, skew angle and model scale on scour is almost similar for any kind of sand. However, scour depths and widths are proportional to the square root of the critical tractive force of the sands, if the experiments are performed under critical conditions for the same bed slope and for the same time period.

iv) For the same sand, the scour is less when the depth of flow is less, but the rate of decrease is related to the characteristics of the sand, the pier shape and the model scale.

6. A study on the mechanics of scour caused by bridge pier

(26) General

Since a perfect conclusion on the mechanics of scour has not been established, the author briefly describes the studies made by Keutner and Tison and also gives his opinion on his own study.

A. Keutner's study

The pattern of flow around a wall type pier is shown in Fig. 68. In Fig. 68 the fine solid line is the water surface before inserting the pier, and the thick solid line (1) shows the water surface along the pier wall and the thick dotted line (2) shows the water surface along the center line of the path of flow after inserting the pier. The following facts are observed from Fig. 68.

i) The stagnation depth h_s decreases with a decrease in the nose angle 2α. The water surface along the pier wall drops at point F and the steep slope I' between S and F has a remarkable effect on the scour. The water surface for a pier having an angle of skew to the flow is different for the right and left side of the pier, and this difference becomes more evident as the skew angle gets larger.

ii) Water surface (2) begins to drop at point S_o, far beyond point S, and its height h_o is small compared to h_s. The value of h_o is almost independent of the nose and tail shape. Nevertheless, the distance between S and S_o, which is affected by the pier nose, decreases with a decrease in the nose angle 2α and it seems to be proportional to the velocity difference, $V_i - V_o$, between profiles (1) and (2). Fig. (69) (a) shows the measured water surface. From this figure the lateral slope is recognized as shown in Fig. 69 (b). This lateral slope is evident for a pier having skew angle as shown in Fig. 70.

Engels and many other experimenters showed that this lateral slope causes vertical eddies and these eddies, when associated with the bottom flow, scour the bed material. The lateral slope is closely related to the shape of the pier nose and the scour is related to the lateral slope, hence, the scour is controlled by the nose shape. The eddy motion is shown in Fig. 69 (d). Eddy 1) results from the inverse slope at point S and scours the bed of the nose in the upstream direction. Eddy 2) results from the lateral slope I' and scours the bed along the pier wall in the downstream direction. Between these

numerous
two eddies, there are several eddies that cause scour as shown in Fig. 69 (c). When 2α is $12^0 \sim 29^0$ the scour caused by eddy 1) is more effective and the pattern is different from that caused by other eddies. t_{max} moves towards point F as 2α decreases from 180^0 to 62.6^0. This is because the point, where the scour effect is most evident, approaches the point F with a decrease of slope I' .

The approximate flow pattern is shown in Fig. 71. The flow separates from points V_e and V_r and flows parallel to the pier wall. At points A_{ur} and A_{ul}, the flow deflects about 6^0 towards the center line of the pier. A vertical eddy called tail eddy occurs in the region S'_r S'_l A'_u and a side eddy occurs in the region $V_e S_e S$. The sand scoured from the nose is piled along the pier wall by the side eddy and at the tail by the tail eddy.

B. Tison's study

The flow pattern for a pier parallel to flow is approximately shown in Fig. 72. Consider a flow net APS lying on a sheet of water parallel to the bed surface and apply the Bernoulli theorem

$$z_A + p_A/\omega_0 = z_S + p_S/\omega_0 - \frac{1}{g}\int_A^S \frac{v^2}{\rho}\,ds$$

where,

z_A, z_S = the height of points A and S measured from a datum plane,

p_A, p_S = pressures at points A and S,

ω_0 = the unit weight of water,

v = velocity of flow,

ρ = the radius of curvature of the streamlines, and

ds = infinitesimal length of curve along AS

If it is assumed that ρ is constant for a point along a vertical section, then $1/g \int_A^S (v^2/\rho)ds$ is smaller on the water sheet which is nearer to the bed surface due to the vlocity being smaller. Accordingly $(Z_s + P_s/\omega_o)$ $-(Z_A - P_A/\omega_o)$ become smaller. For a point A, far from the pier such that $\rho = \infty$, $Z_A + P_A/\omega_o$ is constant along a vertical section. Since $(Z_s + P_s/\omega_o)$ increases from the bed towards the water surface, a vertical acceleration exists. This is contrary to the assumption that the water sheet moves parallel to the bed surface. Actually the water sheet has a downward velocity and scours the bed material. In brief, scour is mainly caused by eccentricity of flow and the nonuniformity of velocity and its magnitude is closely related with $1/g \int_A^S (v^2/\rho)ds$. The following are the results of theoretical consideration.

i) The scour is evident when eccentricity is large. (i.e., radius of curvature of streamline ρ is small)

ii) Upstream piling of sand decreases the scour at the nose. Because the flow pattern is the same as considering the pier nose extending to the pile, the eccentricity of the flow becomes less.

iii) A round pier nose and a sharp tail are effective in decreasing the head loss but not for decreasing scour.

iv) A uniform velocity distribution is much more effective in decreasing scour.

v) The above are based on the assumption that ρ = constant. If ρ changes, it is necessary to consider the change of v^2/ρ.

Tison's experiments were performed in a glass flume (effective length of 1.2 m and a width of 0.7 m) using R. Rhein sand with wooden piers coated with parafin. The depth of flow used was 11 cm and the discharge was 30 l/sec. The experiments illustrated the above statements very clearly. Tison (1939) also stated the difficulties of obtaining a law of similarity for scour around piers in his treatise on dunes and ripples (64).

(27) Author's study

A. General

In general, the water stage of the outer bank in a river bend is high and higher than that of the inner bank scour is observed. Considering this point, the author suggested the similarity between scour at a river bend and scour around piers. If this holds true, it is possible to define the scour mechanics for a pier by analyzing the scour mechanics at a river bend.

In natural rivers, the velocity at the outer bank of the bend is higher than that at the inner bank due to the sand bar low-velocity. For rectangular channels the velocity at the inner bank of the bend is higher than that at the outer banks and this fact has been proved by experiments. Only, at bends, there are secondary currents which move towards the outer bank on the water surface and towards the inner outer bank at the bottom. The secondary currents at the bottom carry sand from the outer bank to the inner bank. As a result of deposition, the depth of water at the inner bank becomes shallow. Also the velocity at the inner bank slows down due to an increase in friction caused by sediment.

B. Scour mechanics at a river bend

The following theoretical studies are for an ideal fluid in a rectangular channel with an arc type bend. The flow at the bend can be considered as a free vortex.

Considering the equlibrium conditions for a water element particle between streamlines AB and CD as in Fig. 73.

$$\left(\frac{w_0}{g}\right) \rho \, d\theta \, d\rho \, dz \cdot \frac{v^2}{\rho} + p \rho \, d\theta \, dz - (p + dp) \rho \, d\theta \, dz = 0$$

therefore,

$$\frac{dp}{w_0} = \left(\frac{v^2}{g\rho}\right) d\rho \qquad \text{(17)}$$

in which,

p = pressure,

v = velocity,

g = acceleration due to gravity

ρ = radius of curvature of streamline, and

w_0 = unit weight of fluid.

If AB and CD lie on a horizontal plan, Bernoulli's theorem can be applied to points P and Q

$$\frac{p}{w_0} + \frac{v^2}{2g} = \frac{p + dp}{w_0} + \frac{(v + dv)^2}{2g}$$

neglecting $(dv)^2$ and substituting into Eq. 17

$$\frac{v \, dv}{g} = -\frac{v^2}{g\rho} d\rho \qquad \therefore \frac{dv}{v} = -\frac{d\rho}{\rho}$$

$$\frac{dv}{v} = -\frac{d\rho}{\rho}$$

Integrating

$$v\rho = c = \text{constant} \qquad \text{(18)}$$

Thus the velocity is inversely proportional to the radius of curvature. Eq. (17) shows that the pressure is high at the outer bank; but, since the pressure at the water surface in an open channel is equal to the atmospheric pressure, this increase of pressure causes a rise in the water surface at the outer bank.

The cross section is shown in Fig. 74 (a). Substituting the term $dP/\omega_o = dH$ into Eq. 17, the lateral slope I_p is

$$I_p = dH/dr = v^2/(gr) \qquad \text{(19)}$$

Combining Eqs. 18 and 19, the height of rise

$$h = \int_{r_1}^{r_2} I_p\, dr = \left(\frac{V_1^2}{2g}\right)\left(\frac{1 - r_1^2}{r_2^2}\right) \qquad \text{(20)}$$

in which v_1 is the velocity at the inner bank.

For viscous fluids, a modification for these equations is required, nevertheless, Eqs 17~20 can be applied for natural flows when the radius of curvature is not very small. Fig. 75 is a comparison between Böss's experimental results and theoretical values computed from the above equations. From the plot it is suggested that the theory for an ideal fluid can be applied to viscous fluids to a certain extent.

Since the velocity distribution in natural rivers is as shown in Fig. 74 (b), it is reasonable to consider that the lateral slope I_p is a result of the main velocity V_m and Fig. 19 is satisfied with the relationship $I_p = V_m^2/g\rho$. However, velocity near the water surface V_s is larger than V_m and in order to have the same I_p-value, ρ_s should be larger than ρ_m. On the contrary, $V_b < V_m$ and ρ_b should be less than ρ_m! According to these reasons, the streamlines where V_s, V_m and V_b are measured and are different in radius. These streamlines are plotted in Fig. 74 (c). Secondary flow in bends originates from this difference in the radius of the streamlines. Secondary currents associated with the main river flow, have a spiral motion and scour the bed material at the outer bank, then, deposit sand at inner bank due to a decrease in velocity at the bottom.

By referring to Hinderks' and Böss' studies, the author explains scour at the outer bank of a river bend and the origin of secondary currents.

The following are the author's opinions on scour caused by secondary flow. Eq. 19 $V_m^2/(g\rho) = I_p$ can be reaaranged as $V_m^2/\rho = gI_p$. Here V_m^2/ρ is the centrifugal force on a unit mass having velocity V_m. This force is balanced by gI_p. However, the centrifugal force V^2/ρ varies with the depth z due to the nonuniform velocity distribution. In order to balance with gI_p, the force $(V^2/\rho - V_m^2/\rho)$ acts towards the outer bank in the region $V > V_m$ and force $(V_m^2/\rho - V^2/\rho)$ acts towards the inner bank in the region $V < V_m$. Accordingly, secondary current is defined as a result of the unbalance of centrifugal force and its intensity is controlled by the following equation.

$$dC = \frac{w_0}{g}\int_{z_m}^{H}\left(\frac{v^2}{\rho} - \frac{v_m^2}{\rho}\right)dz + \frac{w_0}{g}\int_{0}^{z_m}\left(\frac{v_m^2}{\rho} - \frac{v^2}{\rho}\right)$$

in which z_m is the distance from the bed corresponding to the velocity v_m.

According to Lavade-Rapp's formula (78) which is adaptable for velocity distributions in natural rivers

$$\left.\begin{aligned} v = V_s\left(\frac{z}{H}\right)^{1/\alpha} \\ v_m = V_s\left(\frac{\alpha}{\alpha+1}\right) \\ z_m = H\cdot\frac{\alpha}{\alpha+1} \end{aligned}\right\} \quad (21)$$

in which

but when $\frac{H}{V_s} > 2.5$, $\alpha = 1 + 4.80\sqrt[12]{\frac{H}{V_s}}$

and when $\frac{H}{V_s} < 2.5$, $\alpha = 0.818\sqrt[4]{\frac{H}{V_s}}\left(1 + 4.80\sqrt[12]{\frac{H}{V_s}}\right)$

Then

$$dC = \frac{\left(\frac{w_0}{g}\right)\left(\frac{V_m^2}{\rho}\right)H}{\alpha(\alpha+2)}\,d\rho$$

and the intensity of the secondary current is controlled by

$$C = \int_{\rho_1}^{\rho_2} dC$$

Assuming that the scour force is proportional to this value of C

$$K = \phi\frac{w_0}{g}\frac{1}{\alpha(\alpha+2)}\int_{\rho_1}^{\rho_2}\frac{V_m^2 H}{\rho}\,d\rho \qquad \ldots\ldots \quad (22)$$

where

in which,

K = scour force;

V_m = mean velocity;

H = depth of flow;

ρ = radius of curvature of streamlines;

ϕ = experimental coefficient;

r_1 = radius of inner bank;

r_2 = radius of outer bank;

α = roughness of bed, coefficient which is related with $f(H/V_s)$ or H/v_s

Kozeny's proposed α = 5~7; so that

$$\frac{1}{\alpha(\alpha+2)} = \frac{1}{35} \sim \frac{1}{63} ,$$

It is known that either a decrease in channel roughness or an increase in H/V_s can cause a large decrease in the scour.

C. Scour mechanics for bridge piers

As shown in Fig. 72 the stream line changes its direction on both sides of a pier and its flow pattern is considered the same as that of flow in a bend.

The spiral flow occurs due to the nonuniform velocity distribution and scours the bend at the pier nose. If the flow condition pattern is constant, from formula V^2/gr, the scour is mainly controlled by the radius of curvature r of a stream line. Judging from this statement, it is easily understood that scour is closely related to the shape of a pier.

In Fig. 72, Point A is a point where $r = \infty$, i.e., no effect of secondary currents.

Let $d\ell = ds$,

$$\phi \frac{w_0}{g} = \psi ,$$

$$\frac{1}{\alpha(\alpha+2)} = \frac{1}{\sigma} .$$

Then the scour force, K, around the tipe of the nose s is

$$K = \frac{\psi}{\sigma} \int_A^s \frac{V_m^2 H}{r} ds \qquad (23)$$

where ψ is an experimental constant, and

σ is the decrease in channel roughness (increase with H/V_s).

If the scour depth is proportional to the scour force, then the scour depth is proportional to the square of the mean velocity and the depth of flow and inversely proportional to the radius of curvature. Also, the scour will decrease by decreasing the channel roughness or increasing H/V_s.

These coincide with Tison's conclusions and are verified by the author's experiments.

The movement of the scoured particles are shown in Fig. 76. The particles separate from the pier wall making a right angle with the streamline because of spiral flow.

Being affected by the main flow, they move parallel to it. Since, stream lines change in direction towards the pier wall from the transition point F (from now on it will be called reverse eccentricity) the particles move towards the wall due to reverse spiral flow. A part of the particles are carried by vertical eddies. Since the direction of the vertical eddies are opposite to the main flow, the particles are deposited at the wall. According to Karman's boundary layer theory a side eddy is formed when the velocity at the outer side of the boundary layer decreases. For bridge piers, the maximum velocity, V_1, of the flow will decrease after passing the transition point F. This is considered as the main reason for the occurance of side eddies. Therefore, the reverse eccentricity of the flow near the transition point F has a direct relationship with side eddies. As above, the reverse eccentricity pushes the side eddies and the bottom flow towards the pier and, as a result, piling of sand occurs. The same reasoning can be applied to the rear eddies of a pier.

D. Comments on Tison's and Kentener's studies:

Tison and Kentener studied that the scour is caused by horizontal eddies from the tip of the pier nose. This statement coincides with the author's opinion. However, Tison explained horizontal eddies as a result of eccentricity of flow and the nonuniformity of the velocity distribution and Kentener explained it as a result of the lateral slope.

The author supports Tison's statement and gives a discussion for Eq. (16) based on Bernoulli's theorem.

Tison assumed that the energy along each streamline in a sheet of water is constant and also assumed that the water sheet is parallel to the bed surface. Therefore, based on Bernoulli's theorem

$$dz + \frac{dP}{\omega_o} + \frac{v\,dv}{g} = 0$$

or

$$z_A + \frac{P_A}{\omega_o} + \frac{V_A^2}{2g} = z_3 + \frac{P_s}{\omega_o} + \frac{V_s^2}{2g} \quad \cdots\cdots \qquad (24)$$

Eq. (16) can be revised as follows:

The relationship between the centrifugal force and the pressure for the two close streamlines shown in Fig. 72 is $dp/\omega_o = (V^2/g\rho)\,ds$, with an increase in centrifugal force and the water surface rises $dH = dP/\omega_o$ as a result of the pressure increase. The difference of water surface between A and S in Fig. 72 is

$$h_s = \int_A^S \frac{dP}{\omega_o} = \int_A^S \frac{V^2}{g\rho}\,ds \qquad (25)$$

But, in natural rivers, where the velocity distribution is not uniform, it is known that the radius of curvature, ρ, at the bottom should be less than that at the water surface in order to have the same value of h_s.

Consequently a horizontal eddy occurs. The above is a verification of Tison's statement regarding Eq. (16). The occurance of horizontal eddies is explained as a result of a bending of stream lines and nonuniformity of the velocity distribution. Keutner's opinion, that horizontal eddies are due to lateral slope, is basically in error. Keutner explained that the scour at the nose is mainly controlled by the lateral slope I' in Fig. 69 (d). However, the motion of particles, according to observation during experiments, is perpendicular to the pier wall and not parallel to the pier wall, and the eddy corresponding to the lateral slope, I', was not observed.

If lateral slope is the factor which controls the scour, the scour at the seeward side of the flow should be larger than at flowward side for a pier with a skew angle. But, on the contrary, more scour was observed at the flowward side in series $G_1 \sim G_4$. Moreover, the water surface rises parablically around the pier nose and it is difficult to evaluate the lateral slope. For these points, Keutner's opinions are limited in accuracy.

Keutner's opinions almost coincide with author's opinions for the piling-up of sand caused by side eddies and tail eddies. Only the author thinks that it is not reasonable for unstable tail eddies to be considered as dead water and be completely separated from the main flow.

A part of the flow enters the tail eddy region along the pier wall and when this flow meets the flow from the other side of the pier, the stream lines bend at point S'. The phenomenon of this bending of flow is the same as the eccentricity of flow at the top of a pier, so that the water surface rises towards point S' and horizontal eddies carry away a part of the sand which is deposited at the tail. Accordingly, the pile-up on the line of pier axis at the tail is lower than its sides.

E. The relationship between the height of backwater and scour

The scour at a pier nose is due to the horizontal eddies which result from the flow eccentricity and the nonuniformity of the velocity distribution but a rise in stage is only due to flow eccentricity. From this statement, it is seen that there is a basic difference in the mechanics of the two phenomena.

At a bend in a channel, the water surface at the outer bank rises due to an increase in pressure resulting from an eccentric force and, according to Bernoulli's theorem, velocity will decrease.

In the case of a pier, it is clear from Eq. 25 and Eq.23 that the velocity of flow decreases near the tip of a pier and it has an effect on the scour and the rise of stage h_s. Eventually, the degree of flow eccentricity (shape of pier nose) is the main term controlling scour and h_s.

The above discussion, considering the line AS (Fig. 72) upstream from the pier, neglects the effect of velocity changes due to the constriction. However, the drop S_f at point F and the rise h_o at point S_o are affected by the constriction.

The water surface at the outer bank of a bend is higher than at the inner bank. Likewise, the water surface at the tip of a pier is high and it will drop at the transition point due to a reverse bend in the flow. As a matter of fact, the drop of water surface at point F is also due to an increase in velocity caused by the constriction . The value of the drop S_f decreases when the opening ratio of the channel is large and if the opening ratio is constant, S_f is controlled by the pier shape. The sharper the pier nose the less the S_f will be. Considering the water surface (2) shown in Fig. 68, the water surface, upstream from the tip of a pier, rises due to a decrease in velocity resulting from flow eccentricity and this tendency increases at point F due to a decrease in velocity resulting from flow eccentricity and this tendency increases at point F due to a reverse bend in the flow. However, the water surface drops lower than the water surface (1) due to a velocity increase resulting from the constriction. This effect extends a considerable distance upstream of the pier. The rise h_o at the point S_o in Fig. 68 is due to these two effects and it is naturally less than h_s at point S . When to decrease the rise of water surface, the pier nose is sharpened, h_o is not affected by the pier shape because point S_o approaches S. The above discussion neglects the friction loss of the flow and also the losses due to the side eddies and the tail eddies. In general, wave move towards the upstream in subcritical flow and since the flow downstream is steady with a constant depth, the rise of water surface should be equal to the sum of the losses of energy for a corresponding distance. The loss is evident at the tail of a pier. Therefore it is necessary

to consider the effect of the tail shape on scour. If the water surface rises upstream of a pier, the mean velocity V_m decreases due to an increase in the depth of flow, H_o. According to Eq.23, the scour will decrease but its value is comparitively small.

(28) Author's opinion regarding the law of similarity for scour experiments:

Scour is related to pier shape, model scale, critical conditions and the characteristics of the bed material. Although it is difficult to obtain quantitative conclusions from the experimental result, but, approximate quantitative conclusions can be established by a clear understanding of the mechanics of scour around piers.

The author assumed that the scour from K (Eq.23) was a direct controlling factor for scour depth and scour width, and proposed the following equations:

$$\left.\begin{aligned} k_o &= \xi K \\ t_s &= \eta K \end{aligned}\right\} \qquad (26)$$

where: ξ and η are experimental constants. But scour width K_f and scour depth t_f at the point F is difficult to predict due to the effects of other factors such as sand pile-up resulting from vertical eddies etc.

Assuming Eqs. 23 and 26 can be applied for K_o and t_s, and letting the vertical scale be 1/n and the horizontal scale be 1/m.

Here the prime sign (') is for natural channels. Substituting H into R,

since $H = nH'$ and

$$I = \frac{n}{m} I' ,$$

$$\frac{V}{V'} = n^{M-1} m^{-1/2} n^{7/6} \qquad (27)$$

in which n_M^{-1}, ν, ν', N, N', E

but $nm = n/n' = n_M$

Substituting into eqs. 23 and 26 and letting $\rho = m\rho$ and $ds = mds'$, Eq. 27

$$\frac{K}{K'} = \left(\frac{\psi}{\psi'}\right) n_M^{-2} m^{-1} n^{10/3} \qquad (28)$$

$$\frac{k_0}{k_0'} = \left(\frac{E}{E'}\right)\left(\frac{\psi}{\psi'}\right) n_M^{-2} m^{-1} n^{10/3}$$

$$\frac{t_s}{t_s'} = \left(\frac{\eta}{\eta'}\right)\left(\frac{\psi}{\psi'}\right) n_M^{-2} m^{-1} n^{10/3} \qquad (29)$$

σ, σ'

Considering different bed materials and using Kramer's formula Eq. 10,

$$f_0 = \frac{F_0}{F_0'} = \frac{e\nu}{\mu} = \frac{n^2}{m^2},$$

therefore,

$$e = \frac{n^2 \mu}{m \nu} \qquad (30)$$

in which $e = d_m/d_m'$, $\mu = M/M'$ and $\nu = (w - w_0)/(w' - w_0)$.

If natural sand is used for the experiments and its sieve analysis is similar to that of a natural river sand then

$$\mu = 1 \quad \text{and}$$

$$\nu = 1$$

Eq.30 becomes

$$f_o = e = \frac{n^2}{m} \qquad \cdots\cdots \qquad (30_{\frac{1}{2}})$$

Thus the law of similarity can be established from Eqs. (28) ~ (30'). However, the determinations of the experimental coefficient ψ, ξ, η and α are still a great problem.

Assuming there is no visible differences for these values between model and natural river, then $\frac{\psi}{\alpha} / \frac{\psi'}{\alpha'} = 1$, $\xi/\xi' = 1$ and $\eta/\eta' = 1$, moreover, applying Vogel's proposal of $n_M = N/N' = 1$. A simple formula can be obtained as follows:

$$\frac{k_o}{k_o'} = \frac{t_s}{t_s'} = m^{-1} \eta^{10/3} \qquad \cdots\cdots \qquad (31)$$

in which

put in $e = \frac{(n^2 \mu)}{(m \nu)}$

or, $e = \frac{n^2}{m}$

Since the purpose of this report is to obtain qualitative conclusions for scour around piers, it is regretable that the data from the experiments cannot verify the equations given above. For example, the necessary critical conditions for discussing the relationship between K_o' and t'_s and K_o and t_s for experiments described in Sec. (22) are tabulated in Talbe 46. In which $e = n^2/m = 1$ because the same sand is used for the experiments. Nevertheless, all the experiments were performed under the same critical conditions, with depth of flow as 5.2 cm and slope as 1/200. For these reasons, the data from the experiments cannot be used for discussing quantitative conclusions.

With an increase in the depth H , the mean velocity V_m decreases. Judging from Eq 23, the scour will decrease very slightly, and, according to Eq 25, rise of water surface decreases. So that the water surface rise from the original water surface, h_s , is not much.

Since h_s is nearly constant, S_f decreases with an increase H . However, because h_s itself is comparatively large, this effect is not evident in the value of h_s . However, depth of flow has a large effect on h . For this reason h_o is affected by both the side eddies and the tail eddies. Rehbock defined back-water as a water surface rise at the point which is a distance equal to the pier length upstream from pier tip. Although his definition is not the same as h_o , based on the above explanation, he evaluated the great effect of tail shape on scour (Ref. 11). As stated before, it is known that the scour and h_s are mainly controlled by the nose shape, whereas, S_f is mainly controlled by the nose shape and the change in velocity due to the constriction ~~by the nose shape and the change in velocity due to the constriction~~. These facts doincide with Keutner's study (26) and can be verified from the values of h_s and S_f in Table 45. The tail shape has a large effect on h_o . However, for the author's experiment, this effect was not observed due to the shallow depths of flow, also all h_o - values measured were less than 1 mm .

7. Conclusions

Chapter 1 ;

With the development of transportation, bridge construction, especially the sub-structures (pier), have become important subjects. Accordingly, it

is necessary to evaluate the scour around piers, which control the stability of a bridge. However, it is difficult to study this subject from the view-point of theoretical fluid mechanics, so that, experimental studies reported in this report were to obtain qualitative conclusions which could be applied in the field.

Chapter 2 :

The author stated the necessity of comparing the impulse theory and the tractive force theory for the stability of a bed surface. Welikanoff studied the problem from the view-point of the impulse theory that his results are not applicable in this field.

The tractive force theory was proposed by DuBoys, and further refined by Kramer and Yasu. The author recognizes the reliability of this theory and uses it as a foundation for his experiments.

Based on the tractive force theory, the author developed a law of similarity for pier scour, however, only qualitative conclusions could be obtained.

By preliminary experiments, it was proved that a particular bed material has a constant critical tractive force. The main experiments were performed under the critical conditions obtained through the preliminary tests. Thus the scour is assumed to be a result of the existance of piers.

Chapter 3 :

Scour is largely affected by pier shape, and the stability of a pier is mainly controlled by scour at the nose. The author discussed his experimental results and hydraulically explained the scour at the nose as a result of eccentricity of flow.

The scour at the nose is independent of the length of a pier and the tail shape. The backwater and the dynamic pressure on a pier are controlled by side eddies and tail eddies, accordingly, they will decrease by sharpening the nose and tail rather than the nose.

A two circular pier bridge is not advisable and in the case this type of bridge is not advisable, the distance between the two piers (c. to c.) is recommended to be twice the pier diameter.

Chapter 4 :

In general, the scour for a pier having a skew angle to flow increases with the angle and the rate of increase varies with pier shape. From experiments, it is known that the rate of increase is much less for a pier having a rounded nose and tail. A measureable increase in scour between two piers was observed for the two circular pier type bridge with a skew angle and, with an increase in the skew angle, each pier begins to act as an individual pier.

The effect of the opening on the scour is very slight, when the opening ratio is very large, and only when the opening ratio is less than 10 ~ 15% this effect becomes evident.

The author also suggests methods of construction for new bridges built near existing ones.

Chapter 5 :

In order to obtain results applicable to the field the author discussed the effect of model scale. Judging from the experimental data, it is known that as the model scale 1/n approaches zero (no pier) the bed scour also

approaches zero. From this fact, the author's experimental results can be used as a guide for qualitative suggestions on scour in the field. Since the effects of pier shape, skew angle, and model scale on scour are similar for all kinds of bed material, the experimental results given in Chapters 3 and 4 are qualitatively reliable for applying to field cases.

Chapter 6 :

By assuming the scour phenomena at a pier nose is similar to the scour phenomenon at a river bend, the author stated that scour results mainly from horizontal eddies caused by eccentricity of flow and nonuniformity of velocity along a vertical section. Accordingly, it is reasonable to consider that the effect of pier shape and pier arrangement, for a particular critical condition, are controlled by eccentricity of flow at the pier.

However, it is difficult to obtain quantitative conclusions from the experimental data given in this report.